Atlantic Geology

Precise U-Pb ages for the cogenetic alkaline Mount LaTour and peraluminous Mount Elizabeth granites of the South Nepisiguit River Plutonic Suite, northern New Brunswick, Canada

Zeinab Azadbakht, Christopher R.M. McFarlane et David R. Lentz

Volume 52, 2016

URI : https://id.erudit.org/iderudit/ageo52art07

Aller au sommaire du numéro

Éditeur(s)

Atlantic Geoscience Society

ISSN

0843-5561 (imprimé)
1718-7885 (numérique)

Découvrir la revue

Citer cet article

Azadbakht, Z., McFarlane, C. R. & Lentz, D. R. (2016). Precise U-Pb ages for the cogenetic alkaline Mount LaTour and peraluminous Mount Elizabeth granites of the South Nepisiguit River Plutonic Suite, northern New Brunswick, Canada. *Atlantic Geology*, *52*, 189–210.

Résumé de l'article

Le cortège plutonique de la rivière Nepisiguit Sud consiste en diverses phases de roches plutoniques felsiques à mafiques dont l'origine remonte au début du Dévonien dans le nord-est du Nouveau-Brunswick. La fraction felsique de ce cortège intrusif est composée d'un vaste pluton de granite à biotite homogène et hyperalumineux (le granite du mont Elizabeth), flanqué sur le versant ouest par le granite alcalin du mont Latour. De nouvelles analyses in situ et la géochronologie U-Pb sur minéraux séparés par spectrométrie de masse à plasma à couplage inductif à ablation au laser (LA-ICP-MS) de la monazite et de grains de zircon issus des deux versants du cortège ont établi un âge de cristallisation de 417,3 ± 0,96 Ma pour le granite du mont Elizabeth et de 417,7 ± 4,4 Ma pour le granite du mont Latour. Les nouvelles données viennent confirmer des études géochronologiques antérieures et indiquent une relation temporelle étroite entre les phases felsiques du cortège plutonique.

[Traduit par la redaction]

Precise U-Pb ages for the cogenetic alkaline Mount LaTour and peraluminous Mount Elizabeth granites of the South Nepisiguit River Plutonic Suite, northern New Brunswick, Canada

Zeinab Azadbakht*, Christopher R.M. McFarlane, and David R. Lentz

Department of Earth Sciences, University of New Brunswick, P.O. Box 4400, Fredericton, New Brunswick E3B 5A3, Canada

Corresponding author <zeinab.azadbakht@unb.ca>

Date received: 13 April 2016 ¶ Date accepted: 13 September 2016

ABSTRACT

The South Nepisiguit River Plutonic Suite consists of various phases of felsic to mafic plutonic rocks of early Devonian age in northern New Brunswick. The felsic portion of this intrusive suite includes a large pluton of homogeneous, peraluminous biotite granite (the Mount Elizabeth Granite), which is flanked on its western side by the alkaline Mount LaTour Granite. New in situ and mineral separate U-Pb Laser Ablation-Inductively Coupled Plasma Mass Spectrometry analyses of monazite and zircon grains from both sides of the suite define a crystallization age of 417.3 ± 0.96 Ma for the Mount Elizabeth Granite and 417.7 ± 4.4 Ma for the Mount LaTour Granite. The new data confirm previous geochronological work and indicate a close temporal relationship between these felsic phases of this plutonic suite.

RÉSUMÉ

Le cortège plutonique de la rivière Nepisiguit Sud consiste en diverses phases de roches plutoniques felsiques à mafiques dont l'origine remonte au début du Dévonien dans le nord-est du Nouveau-Brunswick. La fraction felsique de ce cortège intrusif est composée d'un vaste pluton de granite à biotite homogène et hyperalumineux (le granite du mont Elizabeth), flanqué sur le versant ouest par le granite alcalin du mont Latour. De nouvelles analyses in situ et la géochronologie U-Pb sur minéraux séparés par spectrométrie de masse à plasma à couplage inductif à ablation au laser (LA-ICP-MS) de la monazite et de grains de zircon issus des deux versants du cortège ont établi un âge de cristallisation de 417,3 ± 0,96 Ma pour le granite du mont Elizabeth et de 417,7 ± 4,4 Ma pour le granite du mont Latour. Les nouvelles données viennent confirmer des études géochronologiques antérieures et indiquent une relation temporelle étroite entre les phases felsiques du cortège plutonique.

[Traduit par la redaction]

INTRODUCTION

The South Nepisiguit River Plutonic Suite (SNRPS) is a group of spatially related felsic and mafic plutons in northern New Brunswick (Fig. 1). The SNRPS comprises a dominant phase of peraluminous biotite granite (Mount Elizabeth Granite) to the east, several smaller plutons of alkaline granite, including the Mount LaTour Granite, to the west, and scattered mafic stocks and plutons (Wilson 2013a; Fig. 1). The Mount Elizabeth Granite is the most aerially extensive phase of the SNRPS (Fyffe 1971; Whalen 1993), and has previously yielded a U-Pb (monazite) age of 417 ± 2 Ma (Bevier and Whalen 1990); however, an imprecise age obtained from the Mount LaTour Granite (414 +11/-1 Ma; Bevier and Whalen 1990) leaves some uncertainty as to whether it is coeval with or younger than the Mount Elizabeth Granite. In an earlier study, biotite grains from the Mount Elizabeth Granite yielded the highest Sn, W, Mo, and Sb among all the studied samples of Acadian intrusions of New Brunswick (Azadbakht *et al.* 2015). This fact motivated the authors to investigate the temporal relationship between different phases of SNRPS to further study the possibility of granophile mineralization within this plutonic suite. The purpose of this paper is to report new in situ U-Pb monazite and zircon ages for the Mount LaTour Granite, and both in situ monazite and

0843-5561|16|00189-210 $4.30|0

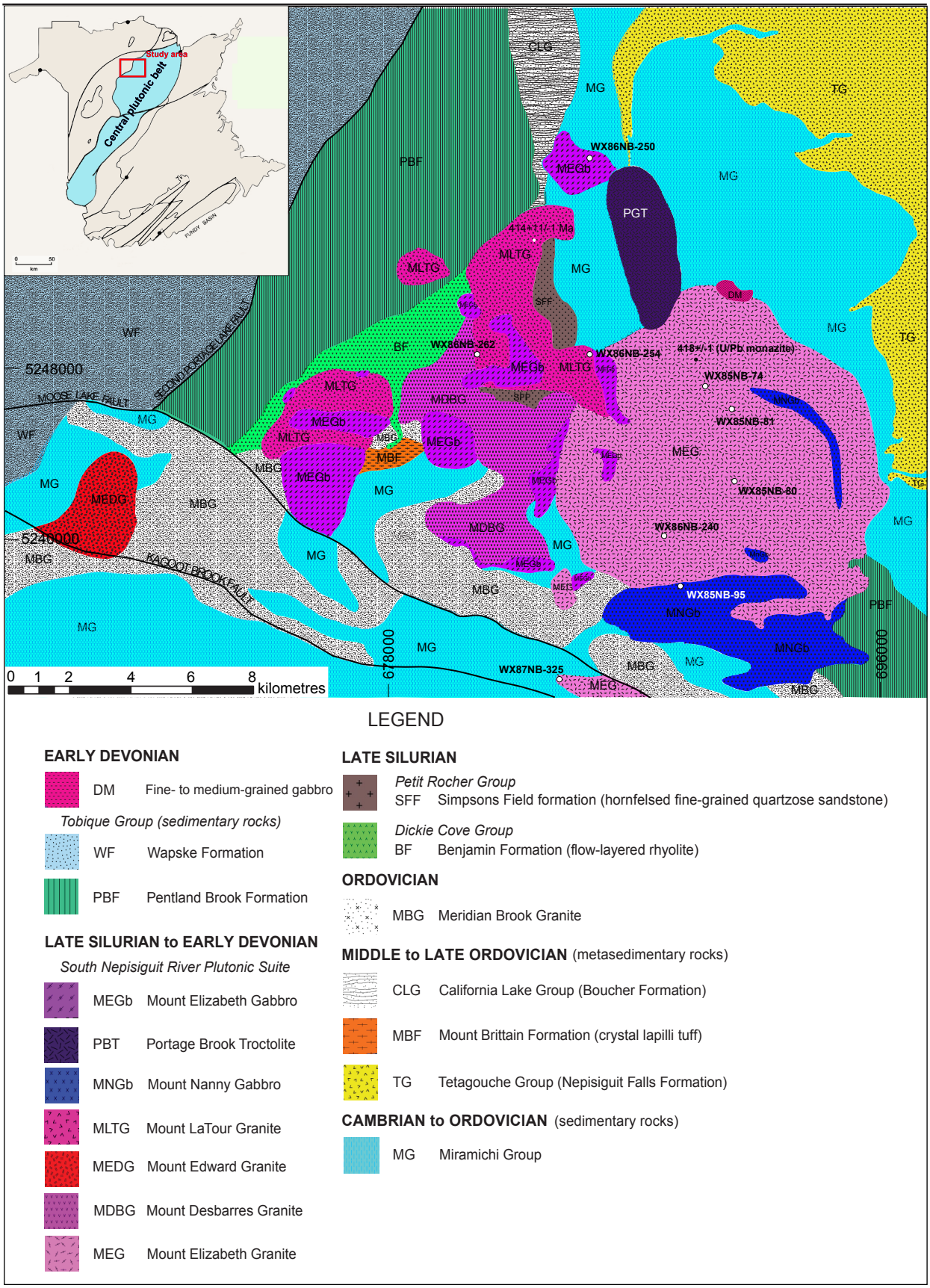

Figure 1. Geological map of the South Nepisiguit River Plutonic Suite in northern New Brunswick modified after Wilson (2013a, b) and Fyffe *et al.* (2011). Sample locations are from Whalen (1993).

zircon mineral separate ages for the Mount Elizabeth Granite, based on Laser Ablation-Inductively Coupled Plasma Mass Spectrometry (LA-ICP-MS).

GEOLOGICAL SETTING AND FIELD RELATIONS

The SNRPS is a part of the Central plutonic belt of New Brunswick (Fig. 1 inset). This belt extends from Chaleur Bay in northeastern New Brunswick southwestward to the American border and into adjacent Maine (Wilson and Kamo 2008). It includes numerous calc-alkaline, foliated and non-foliated Silurian-Devonian granitic intrusions, which intruded the Bathurst Supergroup, Cambrian to Early Ordovician rocks of the Miramichi, Woodstock, and Meductic groups, and the Trousers Lake metasedimentary Suite (Wilson and Kamo 2016).

The SNRPS underlies a roughly circular area of about 400 km^2 in northern New Brunswick. It mainly intruded sedimentary rocks of the Cambrian-Ordovician Miramichi Group, and volcanic and sedimentary rocks of the Middle Ordovician California Lake Group, but the western alkaline phases also intruded Ludlovian to Lochkovian rocks of the Petit Rocher and Tobique groups (Fig. 1; Wilson 2013a). The enveloping contact metamorphic aureoles contain cordierite and andalusite up to 1.5 km from the contact (Whalen 1993; de Roo and van Staal 1994).

Fyffe *et al*. (1981) introduced the name Mount Elizabeth Granite, whereas Whalen (1993) referred to the Mount Elizabeth Intrusive Complex, which he divided into peraluminous granite, alkaline granite, and mafic suites. The large, eastern pluton of peraluminous granite (Mount Elizabeth Granite) is flanked to the west by the alkaline granite suite (Mount Des Barres Quartz Monzonite, Mount LaTour Granite, and Mount Edward Granite); all felsic phases are intimately associated with scattered plutons and small stocks of mafic intrusive rocks, including the Portage Brook Troctolite (dark green, medium- to coarse-grained layered troctolite), Mount Manny Gabbro (dark green medium- to coarse-grained, equigranular to porphyritic gabbro, diorite, and diabase), and several small mafic intrusions collectively referred to as the Mount Elizabeth Gabbro (fine- to medium-grained equigranular to plagioclase-phyric diabase, medium- to coarse-grained gabbro, and minor diorite and quartz diorite)(Whalen 1993). Contact relationships between the Portage Brook Troctolite and other intrusive phases have not been observed; however, relationships between other mafic intrusions and the granitic phases, such as cuspate, irregular contacts and evidence of hybridization along contacts, suggests that they are essentially contemporaneous (Whalen 1993).

The Mount Elizabeth Granite consists of compositionally and texturally homogeneous, pink and white, equigranular, fine- to coarse-grained biotite granite that locally contains minor muscovite (Whalen 1993). Field observations reveal that, in places, the alkaline phases exhibit marked heterogeneity at the outcrop scale (Whalen 1993). However, contacts between the alkaline and peraluminous phases, and among the alkaline phases, have not been observed. The most extensive and most fractionated unit is the Mount Latour Granite, a scarlet red, medium- to coarse-grained, equigranular granite. The Mount LaTour Granite is amphibole bearing, and much of it contains only one feldspar (i.e., hypersolvus granite; Whalen 1993). The nomenclature used herein is taken from the New Brunswick lexicon of bedrock geology (New Brunswick Department of Energy and Resource Development 2016) and the most recent bedrock geology maps (Wilson 2013a, b)

PREVIOUS ISOTOPIC DATING

Bevier and Whalen (1990) reported Thermal Ionization Mass Spectrometry (TIMS) U-Pb zircon and monazite ages for the Mount Elizabeth Granite and a TIMS U-Pb zircon for the Mount LaTour Granite. They reported $^{207}Pb/^{235}U$ ages for monazite to avoid anomalous $^{206}Pb/^{238}U$ ages resulting from higher than expected ^{230}Th disequilibrium in these young rocks.

In the Mount Elizabeth Granite, the results for zircon and monazite grains are not in a complete agreement. Duplicate single monazite grains yielded a $^{207}Pb/^{235}U$ age of 418 ± 1 Ma; whereas, one zircon is concordant at 416 ± 1 Ma. Therefore, an average age of 417±2 Ma was assigned to the intrusion by Bevier and Whalen (1990).

In contrast, Mount LaTour zircon grains are discordant and show evidence of an inherited xenocrystic component. Bevier and Whalen (1990) introduced the lower intercept of 414 +1/-11 Ma as the best estimate of the age of emplacement for this intrusion. They concluded that the upper intercept (ca. 2.7 Ga) gives an average age for the inherited component.

SAMPLING AND ANALYTICAL METHODS

The uncertainties related to the crystallization age and petrological differences among the subunits of the SNRPS encouraged the authors to re-examine the ages of different units in the intrusive suite using in situ and mineral-separate U-Pb monazite and zircon dating at the LA-ICP-MS lab at the Department of Earth Sciences, University of New Brunswick.

The study was conducted in two stages, using archived samples from the study conducted by Whalen (1993): (1) three standard polished thin sections, one from the Mount Elizabeth Granite (WX86NB-240), and two from the Mount LaTour Granite (WX86NB-254, and -262) were selected for in situ LA-ICP-MS analysis; and (2) seven samples (WX85NB-74, 80, 81, 95, WX86NB-240, 250, and WX87NB-325) from the Mount Elizabeth Granite were sent for heavy mineral separation and the resulting monazite and zircon grains were examined and dated. Sample locations are shown in Figure 1. Two of the Mount Elizabeth samples (WX85NB-95 and WX86NB-250) are

not located in the main body of the pluton, but occur as dykes or enclaves of granite hosted by gabbro to the south and north, respectively, of the Mount Elizabeth Granite (Fig. 1). The ages obtained during the two analytical stages were compared in order to establish the best crystallization age of each rock unit. The seven samples from the Mount Elizabeth Granite are medium- to coarse-grained, equigranular pink to white biotite granite, whereas Mount LaTour sample WX86NB-254 is coarse-grained biotite granite, and sample WX86NB-262 is coarse-grained, equigranular, biotite-amphibole alkaline granite. The seven samples of the Mount Elizabeth are similar mineralogically, and have biotite as the main mafic phase accompanied by traces of muscovite. Mineralogical data for the studied samples from Whalen (1993) are provided in Table A1 in Appendix A.

In stage one, monazite and zircon grains were studied with scanning electron microscope back-scattered electron (SEM-BSE) imaging, and selected grains were subsequently dated by LA-ICP-MS. Samples WX86NB-240 and -254 contain both monazite and zircon, whereas sample WX86NB-262 has only zircon (Appendix B; Figs. B1, B2). In total, five monazite and nineteen zircon grains were analyzed from these samples during the first stage of this study. Zircon grains are more fractured than monazite grains in the samples examined. Euhedral monazite grains in sample WX86NB-240 are large (average 50 μm × 30 μm) and zoned, whereas monazite in sample WX86NB-254 is subhedral and measures 240 μm × 100 μm. Zircon grains are commonly euhedral to subhedral and display oscillatory zoning. Grains are greater than 50 μm in the long direction, and some show evidence of secondary metamictization and alteration. In such cases, the least altered part of the grain was analyzed. Most of the zircon grains display metamorphic overprints in SEM-BSE, and some show evidences of a narrow secondary regrowth. However, the regrowth layers were not thick enough to be targeted with the laser beam. As a result, rock samples were sent for mineral separation to provide more clear grains to choose from and to study in more detail potential overgrowths. In the monazite runs, the GSC-8153 monazite was used for external calibration, whereas the 44069 (Delaware) monazite (U-Pb ID-TIMS age of 424.9 ± 0.4 Ma; Aleinikoff *et al.* 2006) was analyzed as a secondary standard. In the case of zircon analysis (both stages), standard FC-1 (Paces and Miller 1993) was used as the zircon reference standard and the Plesovice standard (weighted mean $^{206}Pb/^{238}U$ ID-TIMS date of 337.13 ± 0.37 Ma; Sláma *et al.* 2008) used as a secondary standard.

For the second stage of dating, heavy minerals were separated from the seven samples of Mount Elizabeth Granite using electric pulse disaggregation at Overburden Drilling Management Limited in Ottawa, Canada. Heavy mineral concentrates of all samples examined in stage two have abundant, large (>500 μm) grains of both zircon and monazite. Clear, elongate, euhedral to subhedral crystals of monazite and zircon with internal concentric zoning and minimal mineral inclusions were handpicked and mounted. The textures and morphology of the mounted crystals were studied, and imaged by transmitted light and by cathodoluminescence (CL) imaging. Zircon grains were first dated by LA-ICP-MS in an unpolished grain mount in order to sample only the outermost overgrowths and to avoid xenocrystic cores. The puck was then polished, and further SEM-BSE imaging was done to study the textures in detail (Appendix B; Fig. B3). Visible overgrowths were then targeted for the final stage of the second phase. Ablation was conducted using a Resonetics M-50-LR 193nm Excimer laser ablation system described by McFarlane and Luo (2012) and following methodologies outlined in McFarlane (2015). Standards employed are as described above for both stages. Standards and unknowns were ablated with 24 μm diameter craters for zircon and 13 μm (stage one), and 17 μm (stage two) diameter craters for monazite using a repetition rate of 3 Hz. Typical ablation time was 30s, with 30s background collection.

The data from both analytical stages were reduced offline using the VizualAge U-Pb geochronology plugin running under Iolite v. 2.5 (Paton *et al.* 2011; Petrus and Kamber 2012). VizualAge incorporates a ^{204}Pb-based common-Pb correction that is suitable when the net ^{204}Pb ion beam is measured with sufficient precision (typically <20% 1σ). Concordia ages and weighted mean $^{206}Pb/^{238}U$ ages were calculated using Isoplot version 3.71.09.05.23nx (Ludwig 2009). Data were first filtered by common-Pb content to consider those with ~99% Pb* (radiogenic Pb). Then the data were filtered to consider points that are less than 1% discordant. The procedure resulted in a cluster of data and concordia ages were calculated for clusters of 3 or more concordant data that overlap within error. Inverse isochron lower intercept ages were also calculated for comparison where high common lead levels precluded accurate ^{204}Pb-based correction.

The accuracy of monazite data was confirmed by a concordia age of 422.2 ± 3.2 Ma (MSWD = 1.04, probability of fit = 0.31, in situ), and 424.0 ± 2.4 Ma (MSWD = 0.83, probability of fit = 0.36; heavy mineral concentrate) measured on the 44069 standard. Furthermore, the accuracy of zircon data is confirmed by a concordia age of 339.3 ± 2.7 Ma (MSWD = 0.59 probability of fit = 0.44, in situ), and 337.7 ± 2.0 Ma (MSWD = 1.7, probability of fit = 0.19, heavy mineral concentrate) measured for the Plesovice standard.

MONAZITE DATA: RESULTS AND INTERPRETATION

In situ data collected from samples WX86NB-240 (Mount Elizabeth Granite) and -254 (Mount LaTour Granite) show no evidence of inheritance (Table 1). Monazite grains from sample WX86NB-240 yielded thirteen near-concordant spots overlapping within uncertainty and defining a concordia age of 417.6 ± 2.2 Ma (MSWD = 0.47, probability of fit = 0.50; Fig. 2a); the same set of analyses yielded a

Table 1. Laser ablation ICP-MS data for in situ monazite from two phases of the SNRPS.

Spot name		Y (ppm)	Th (ppm)	U (ppm)	U/Th	$^{206}Pb/^{204}Pb$	†%Pb*	$^{207}Pb/^{235}U$	2σ	$^{206}Pb/^{238}U$	2σ	err. corr.	$^{207}Pb/^{235}U$	2σ	$^{206}Pb/^{238}U$	2σ	%conc
		Isotope ratios											Ages (Ma)				
Mount Elizabeth Granite (Sample WX86NB-240 UTM: E=688520, N=5241600, Zone 19T)																	
240-M2-1	*	25860	112100	3805	0.034	-3842	99.47	0.50	0.02	0.0672	0.0014	0.26	413	13	420	9	101.7
240-M2-2	*	17600	109000	2964	0.027	-4506	99.70	0.49	0.02	0.0668	0.0015	0.14	409	16	417	9	101.9
240-M2-3		15100	103100	2604	0.025	4163	97.87	0.60	0.03	0.0682	0.0014	0.15	474	16	425	9	89.7
240-M2-4	*	17060	115400	2996	0.026	-20271	99.28	0.51	0.02	0.0671	0.0015	0.38	419	14	419	9	100.0
240-M2-5		25650	108000	3742	0.035	880	97.61	0.64	0.02	0.0686	0.0014	0.26	503	15	428	8	85.0
240-M11-1	*	11900	94700	1683	0.018	-1015	99.29	0.51	0.03	0.0663	0.0015	0.03	419	17	414	9	98.8
240-M11-2		12380	102100	2017	0.020	-2974	98.42	0.59	0.03	0.0702	0.0016	0.10	476	18	438	10	91.9
240-M11-3		14300	87400	1778	0.020	1239	98.10	0.61	0.03	0.0684	0.0015	0.16	483	18	426	9	88.3
240-M11-4		10150	146400	2071	0.014	150	88.87	1.36	0.09	0.0740	0.0018	0.44	870	37	460	11	52.9
240-M13-1	*	23900	102400	3006	0.029	-36375	99.50	0.50	0.02	0.0684	0.0014	0.08	412	14	426	8	103.5
240-M13-2	*	17100	120600	2872	0.024	783	99.48	0.50	0.02	0.0678	0.0014	0.34	411	15	423	9	102.9
240-M13-3	*	18720	122200	3138	0.026	1060	98.61	0.54	0.02	0.0657	0.0013	0.09	434	14	410	8	94.5
240-M13-4	*	20450	104400	2726	0.026	-32500	99.16	0.52	0.02	0.0668	0.0013	0.18	422	15	417	8	98.8
240-M13-5	*	14550	128000	2537	0.020	2308	99.62	0.50	0.02	0.0671	0.0014	0.14	410	16	419	8	102.1
240-M13-6	*	15100	122300	2483	0.020	1884	99.48	0.50	0.02	0.0665	0.0014	0.29	412	15	415	9	100.7
240-M17-1	*	24050	105100	3324	0.032	4842	99.20	0.52	0.02	0.0673	0.0014	0.26	425	16	420	9	98.8
240-M17-2	*	24690	117300	3733	0.032	6055	99.46	0.50	0.02	0.0671	0.0015	0.16	412	14	419	9	101.7
240-M17-3	*	23350	103000	3165	0.031	-1640	99.06	0.51	0.02	0.0665	0.0014	0.20	419	14	415	8	99.1
240-M17-4		33000	101800	4044	0.040	1364	97.75	0.61	0.03	0.0670	0.0014	0.15	484	17	418	8	86.3
Mount LaTour Granite (Sample WX86NB-254 UTM: E = 685440, N = 5247810, Zone 19T)																	
254-M1-1	*	16260	35240	1358	0.039	-5392	99.77	0.48	0.03	0.0666	0.0018	0.33	398	19	416	11	104.4
254-M1-4	*	15580	36360	1360	0.037	1089	99.74	0.47	0.03	0.0662	0.0016	0.21	393	19	413	10	105.1
254-M1-5		12930	84100	1410	0.017	249	92.47	1.54	0.14	0.0975	0.0039	0.86	924	53	599	23	64.8
254-M1-6	*	15020	60600	1159	0.019	-6020	99.49	0.50	0.03	0.0672	0.0015	0.26	411	18	419	9	102.0
254-M1-7		11930	47820	1504	0.031	824	98.49	0.59	0.03	0.0678	0.0018	0.18	465	19	423	11	91.0
254-M1-8	*	15730	31330	1268	0.040	1003	98.92	0.51	0.04	0.0663	0.0019	0.05	413	23	414	12	100.2
254-M1-9		13900	54600	2034	0.037	1632	98.04	0.63	0.03	0.0707	0.0017	0.41	495	19	440	10	88.9
254-M1-10	*	16960	36780	1212	0.033	20333	99.63	0.51	0.03	0.0679	0.0015	0.16	417	21	424	9	101.6
Delaware monazite standard																	
44069-1		29340	28990	4535	0.156	-2297	99.59	0.49	0.02	0.0679	0.0013	0.23	408	13	424	8	103.9
44069-2		23290	28710	5170	0.180	44600	99.72	0.52	0.02	0.0677	0.0013	0.39	421	12	423	8	100.5
44069-3		26460	29600	4791	0.162	3465	99.56	0.52	0.02	0.0680	0.0014	0.12	425	12	424	8	99.7
44069-4		21170	26490	2346	0.089	1077	99.59	0.51	0.02	0.0677	0.0015	0.26	419	15	422	9	100.8
44069-5		21890	25020	2821	0.113	1914	99.22	0.53	0.02	0.0676	0.0013	0.23	433	15	421	8	97.3
44069-6		21490	21590	2374	0.110	-1582	99.75	0.51	0.02	0.0679	0.0015	0.22	419	16	423	9	101.0

* = used for concordia and weighted mean $^{206}Pb/^{238}U$ calculations; † = estimated from Andersen (2002) method; Pb*=radiogenic Pb.

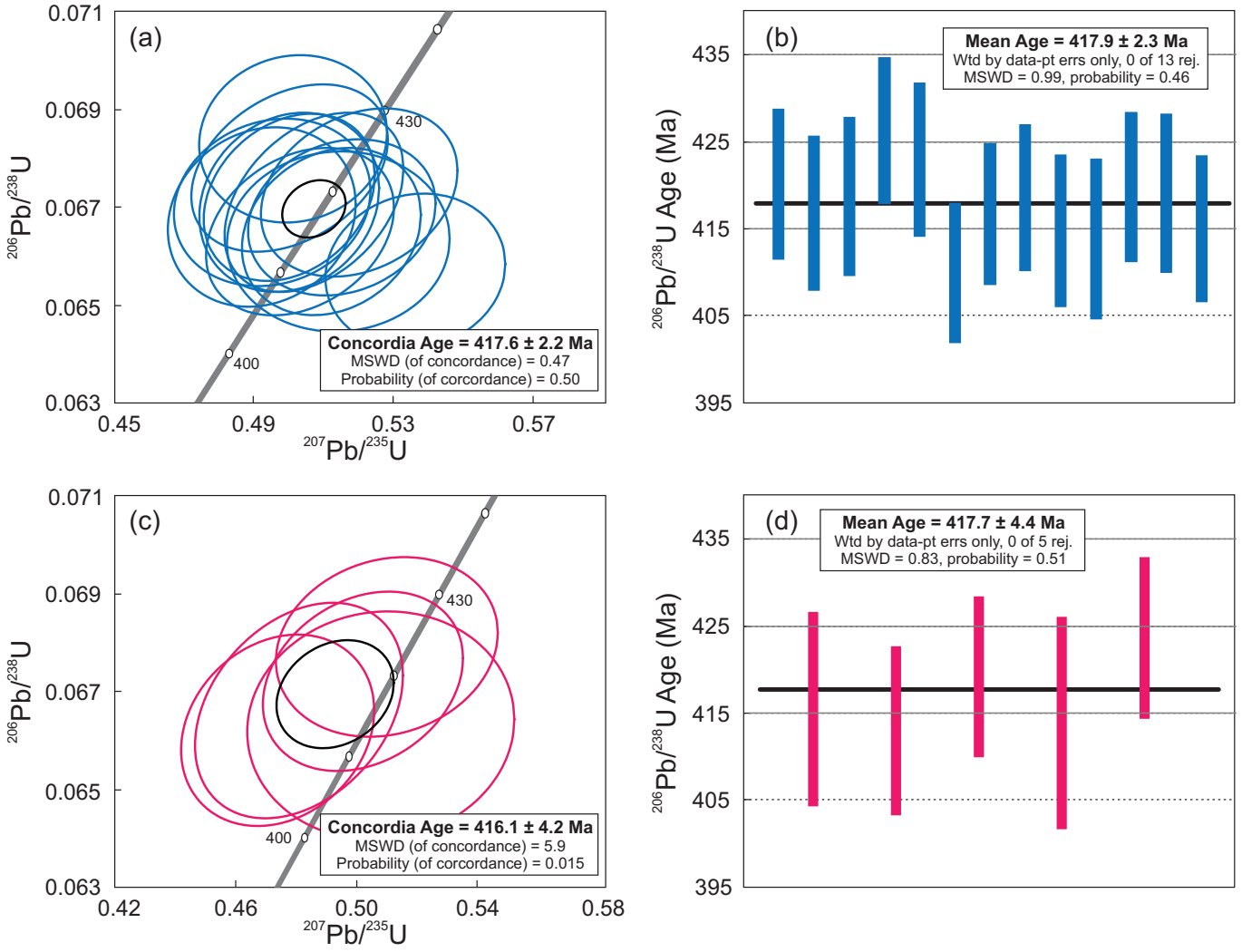

Figure 2. (a) Concordia plot for in situ laser ablation ICP-MS analyses of monazite from the Mount Elizabeth Granite (WX86NB-240). (b) Plot of weighted mean of $^{206}Pb/^{238}U$ ages for monazite grains of the same sample (WX86NB-240). (c) Concordia plot for in situ laser ablation ICP-MS analyses of monazite from the Mount LaTour Granite (WX86NB-254). (d) Plot of weighted mean of $^{206}Pb/^{238}U$ ages for monazite grains of the same sample (WX86NB-254). Error ellipses, and box heights shown at the 2σ level.

weighted average $^{206}Pb/^{238}U$ age of 417.9 ± 2.3 Ma (MSWD = 0.99, probability of fit = 0.46; Fig. 2b). In this study, we interpret the weighted average $^{206}Pb/^{238}U$ dates to represent the best estimate for the crystallization age of each phase. Interestingly, this age is in a complete agreement with the previous dating of Bevier and Whalen (1990). Furthermore, sample WX86NB-254 produced five overlapping, near-concordant analyses that yield a concordia age of 416.1 ± 4.2 Ma (MSWD = 5.9, probability of fit = 0.015; Fig. 2c) with a weighted average $^{206}Pb/^{238}U$ age of 417.7 ± 4.4 Ma (MSWD = 0.83, probability of fit = 0.51; Fig. 2d). This age is within the upper limit of the previous date (414 +11/-1 Ma) obtained by Bevier and Whalen (1990). The two plutons are thus indistinguishable in terms of their monazite $^{206}Pb/^{238}U$ ages, confirming the contemporaneous relationship between the Mount Elizabeth Granite and Mount LaTour Granite as proposed by Whalen (1993). Interestingly Mount LaTour Granite (the westernmost of the three plutons) intruded rhyolite that has an age of 418.6 ± 0.9 Ma (Wilson and Kamo 2008). This may confirm the accuracy of the result indicating the possibility that parts of the plutonic suite have approximately coeval extrusive equivalents.

It is important to note that different reservoirs have different U/Th ratios (0.238, 0.119, 0.228, and 0.500 for the upper crust, lower crust, average crust, and MORB, respectively; Rollinson 1993); as a result, crustal contamination could considerably change the ratio and indirectly affect U/Th in the crystallizing monazite grains. Depending on the time differences between contamination and monazite crystallization, the U/Th ratio of the monazite may reflect either the original magma or a

magma contaminated by assimilation of crustal material. None of the grains from the three samples shows evidence of inheritance; therefore, the U/Th ratios likely reflect the composition of the magma from which they crystallized (i.e., post-crustal contamination).

Similar to the result of the in situ study, the data collected from separated monazite grains of the Mount Elizabeth Granite showed no signs of inheritance (Table 2). Thirty-five monazite grains were ablated, and with the exception of two grains, they define a maximum age cluster at ca. 416 Ma (Table 2). The studied grains yielded eleven near-concordant spots overlapping within uncertainty and resulting in a concordia age of 417.5 ± 2.2 Ma (MSWD = 0.032, probability of fit = 0.86; Fig. 3a); the same set of analyses yielded a weighted average $^{206}Pb/^{238}U$ age of 417.2 ± 3.1 Ma (MSWD = 0.95, probability of fit = 0.48; Fig. 3b). Based on the overlap between the 2σ error envelopes for the results of in situ and separate monazite grains, we assigned an average age of 417.2 ± 1.5 Ma (95% confident) as the best estimate of crystallization age for Mount Elizabeth Granite.

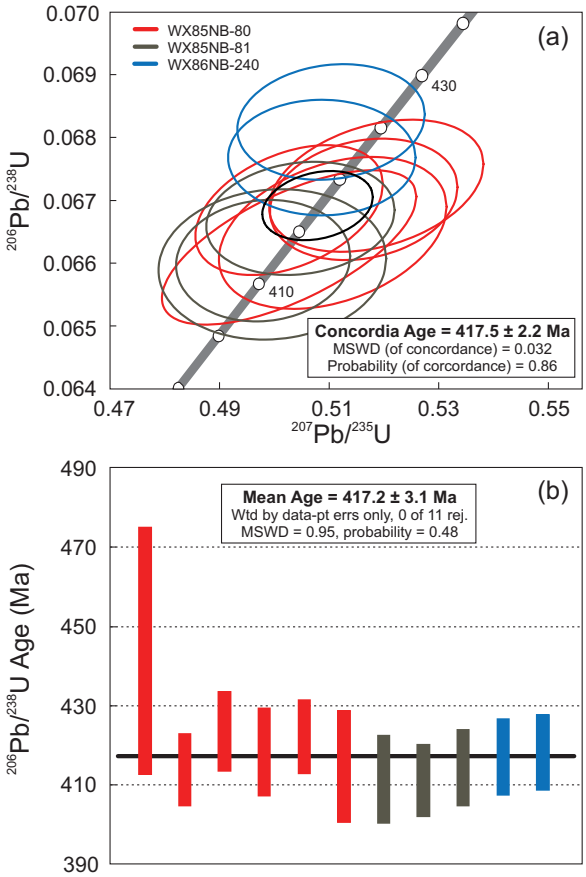

Figure 3. (a) Concordia plot for laser ablation ICP-MS analyses of separated monazite grains from the seven samples of the Mount Elizabeth Granite. (b) Plot of weighted mean of $^{206}Pb/^{238}U$ ages for monazite grains of the same samples. Error ellipses, and box heights shown at the 2σ level.

Table 2. Laser ablation ICP-MS data for separated monazite grains from the Mount Elizabeth Granite.

Spot name		Isotope ratios										Ages (Ma)				
		^{232}Th (ppm)	^{238}U (ppm)	U/Th	$^{206}Pb/^{204}Pb$	†%Pb*	$^{207}Pb/^{235}U$	2σ	$^{206}Pb/^{238}U$	2σ	err. corr.	$^{207}Pb/^{235}U$	2σ	$^{206}Pb/^{238}U$	2σ	%conc
(Sample WX85NB-80 UTM: E = 690660, N = 5242780, Zone 19T)																
80-mz		85200	1857	0.020	1856	99.60	0.57	0.02	0.0681	0.0009	0.19	425	5	456	16	93.1
80-mz-1		101000	6630	0.070	4124	99.72	0.43	0.03	0.0646	0.0010	0.76	403	6	361	18	111.7
80-mz-2		95800	4200	0.040	3315	99.76	0.44	0.02	0.0666	0.0014	0.79	415	9	372	14	111.7
80-mz-3		92200	7530	0.080	11400	99.85	0.47	0.01	0.0629	0.0007	0.20	393	4	394	8	99.7
80-mz-4	*	71300	4830	0.070	282	99.46	0.55	0.04	0.0776	0.0025	0.50	481	15	444	31	108.3
80-mz-5	*	96100	3450	0.040	39929	99.87	0.50	0.01	0.0668	0.0008	0.40	417	5	414	9	100.7
80-mz-6	*	84600	3030	0.040	11143	99.80	0.52	0.02	0.0672	0.0009	0.33	419	5	424	10	99.0
80-mz-7		123100	3650	0.030	13525	99.75	0.49	0.02	0.0653	0.0011	0.15	408	7	403	11	101.2
80-mz-8	*	107400	2840	0.030	3200	99.88	0.51	0.02	0.0665	0.0010	0.34	415	6	419	11	99.1
80-mz-9		83900	5421	0.060	13892	99.84	0.48	0.02	0.0641	0.0008	0.59	401	5	400	11	100.1
80-mz-10		96600	5960	0.060	12929	0.00	0.46	0.01	0.0635	0.0007	0.32	397	4	387	8	102.5
80-mz-11		86200	1970	0.020	1189	99.49	0.44	0.01	0.0676	0.0009	0.58	422	6	370	7	113.8
80-mz-12		101100	5600	0.060	758	99.65	0.42	0.01	0.0654	0.0007	0.68	409	4	356	5	114.7
80-mz-13		81900	4330	0.050	8193	99.87	0.49	0.01	0.0646	0.0008	0.42	404	5	403	10	100.2
80-mz-14		77300	1452	0.020	7381	99.89	0.50	0.02	0.0687	0.0009	0.06	428	5	414	11	103.4
80-mz-15		117800	3923	0.030	933	99.66	0.62	0.03	0.0668	0.0011	0.39	417	7	489	17	85.2
80-mz-16	*	91500	2895	0.030	226300	99.84	0.52	0.01	0.0670	0.0008	0.20	418	5	423	9	99.0
80-mz-17		79300	2330	0.030	583	99.71	0.43	0.01	0.0671	0.0009	0.84	418	5	362	5	115.6
80-mz-18		108200	3201	0.030	11913	99.73	0.49	0.02	0.0640	0.0009	0.25	400	6	406	12	98.5
80-mz-19	*	87300	3720	0.040	2674	99.75	0.50	0.02	0.0663	0.0010	0.66	414	6	415	14	99.6
80-mz-20		116100	5630	0.050	3243	99.73	0.49	0.02	0.0645	0.0011	0.29	403	7	403	13	100.0
80-mz-21		116300	3010	0.030	1240	99.69	0.43	0.02	0.0648	0.0013	0.47	405	8	360	11	112.4
80-mz-22		118700	5600	0.050	4438	99.83	0.46	0.01	0.0616	0.0006	0.14	385	4	387	8	99.6

Table 2. Continued.

Spot name		Isotope ratios										Ages (Ma)				
		^{232}Th (ppm)	^{238}U (ppm)	U/Th	^{206}Pb/^{204}Pb	†%Pb*	^{207}Pb/^{235}U	2σ	^{206}Pb/^{238}U	2σ	err. corr.	^{207}Pb/^{235}U	2σ	^{206}Pb/^{238}U	2σ	%conc
(Sample WX85NB-81 UTM: E = 690590, N = 5245630, Zone 19T)																
81-mz		99580	3332	0.030	2849	99.77	0.55	0.02	0.0669	0.0008	0.36	417	5	443	11	94.2
81-mz-1		99550	4135	0.040	1356	99.79	0.42	0.01	0.0645	0.0008	0.62	403	5	353	6	114.2
81-mz-2		87800	1693	0.020	-42817	99.77	0.53	0.02	0.0675	0.0010	0.11	421	6	429	11	98.2
81-mz-3		96000	2686	0.030	206	99.72	0.54	0.09	0.0702	0.0011	0.72	437	7	430	62	101.7
81-mz-4	*	81800	1840	0.020	3450	99.75	0.50	0.02	0.0660	0.0010	0.08	412	6	412	11	100.0
81-mz-5		82700	2843	0.030	1411	99.77	0.42	0.02	0.0645	0.0010	0.50	403	6	357	11	113.0
81-mz-6		103800	2395	0.020	1120	99.68	0.42	0.01	0.0655	0.0011	0.70	409	7	358	10	114.4
81-mz-7	*	79950	2096	0.030	5163	99.81	0.50	0.01	0.0660	0.0008	0.08	412	5	412	9	100.2
81-mz-8	*	81200	2398	0.030	4482	99.88	0.51	0.01	0.0667	0.0007	0.15	416	4	415	10	100.4
(Sample WX85NB-95 UTM: E = 688910, N = 5239180, Zone 19T)																
95-mz		51130	2581	0.050	184412	99.88	12.18	0.26	0.5037	0.0058	0.77	2629	25	2619	21	100.4
95-mz-1		46900	1161	0.020	45813	0.00	12.49	0.28	0.5117	0.0055	0.59	2663	24	2641	21	100.8
95-mz-2		39500	2365	0.060	181471	0.00	12.87	0.28	0.5193	0.0059	0.59	2696	25	2670	21	101.0
(Sample WX86NB-240 UTM: E = 688520, N = 5241600, Zone 19T)																
240-mz		117500	2424	0.020	549	99.56	0.41	0.01	0.0640	0.0015	0.58	400	9	348	9	114.8
240-mz-1		113500	1959	0.020	924	99.64	0.44	0.01	0.0683	0.0016	0.82	426	9	367	8	116.2
240-mz-2		108100	2200	0.020	2173	99.70	0.55	0.02	0.0686	0.0011	0.12	428	6	445	11	96.2
240-mz-3		81200	6310	0.080	7236	99.84	0.48	0.01	0.0635	0.0009	0.26	397	5	398	9	99.8
240-mz-4	*	83100	2816	0.030	16919	99.89	0.51	0.01	0.0677	0.0008	0.00	422	5	417	10	101.1
240-mz-5		126800	13950	0.110	11317	99.86	0.48	0.01	0.0642	0.0006	0.19	401	4	401	8	100.0
240-mz-6		92400	2530	0.030	2689	99.71	0.54	0.02	0.0679	0.0009	0.18	423	6	440	13	96.2
240-mz-7	*	124400	2798	0.020	3508	99.86	0.51	0.01	0.0682	0.0008	0.13	426	5	419	9	101.7
Delaware monazite standard																
44069		21460	2054	0.100	-4705	99.89	0.53	0.02	0.0690	0.0008	0.13	430	5	429	10	100.3
44069-1		33510	3650	0.110	8717	99.78	0.52	0.02	0.0678	0.0009	0.43	423	6	426	10	99.3
44069-2		31700	4235	0.130	-19114	99.96	0.48	0.01	0.0651	0.0007	0.29	407	4	401	8	101.4
44069-3		23840	2701	0.110	-17223	99.89	0.50	0.01	0.0670	0.0008	0.01	418	5	412	10	101.6
44069-4		29090	2268	0.080	12552	99.85	0.52	0.02	0.0683	0.0008	0.11	426	5	425	10	100.2
44069-5		30770	2715	0.090	-11605	99.91	0.51	0.01	0.0680	0.0008	0.18	424	5	415	9	102.2
44069-6		34550	3430	0.100	14447	99.97	0.49	0.01	0.0674	0.0008	0.30	421	5	403	9	104.3
44069-7		26440	2535	0.100	5191	99.85	0.53	0.01	0.0677	0.0008	0.14	422	5	428	9	98.6
44069-8		25300	3304	0.130		99.83	0.52	0.01	0.0678	0.0008	0.21	423	5	423	9	99.9
44069-9		21140	2587	0.120	6500	99.88	0.52	0.01	0.0686	0.0008	0.09	428	5	426	9	100.6

* = used for concordia and weighted mean ^{206}Pb/^{238}U calculations; † = estimated from Andersen (2002) method; Pb*=radiogenic Pb.

Monazite partitions Th strongly over U into its structure, and the potential effect of ^{230}Th disequilibrium on the ^{206}Pb/^{238}U ratio was calculated using the equation of Schoene (2014). Any correction is strongly dependent on the ratio of Th/U in the mineral relative to the same ratio of the melt, and is annotated by "*f*". If *f* becomes very large, the ^{206}Pb/^{238}U ages will be too old. In the studied samples (seven samples from Mount Elizabeth Granite), the monazite is not very Th rich (Th <13 wt.%; *f* value varies between 0.8713 and 13.4844), with two exceptions, and even with f >10, the impact is manifested in the fourth decimal place for the ^{206}Pb/^{238}U ratio. Therefore, the effect of ^{230}Th disequilibrium is thought to be very small and has almost no impact on the ^{206}Pb/^{238}U ages calculated for the monazite grains. Consequently, 417.2 ± 1.5 Ma is believed to be a good estimate of the true crystallization age of these grains.

ZIRCON DATA: RESULTS AND INTERPRETATION

In situ zircon grains in samples WX86NB-240 (Mount Elizabeth Granite), and WX86NB-254 and -262 (Mount LaTour Granite) were studied with SEM-BSE imaging in order to try to identify overgrowth rims on inherited xenocrysts; however, none of the grains examined showed evidence of overgrowths. This apparent lack of overgrowth is similar to the observation of Roddick and Bevier (1995) for two other Paleozoic granitic intrusions of New Brunswick,

and may indicate a low probability of inheritance in these grains. Furthermore, U-Pb results for each of the samples define discordia suggestive of secondary, low temperature Pb-loss in these grains (also observed by Bevier and Whalen 1990), which is supported by the presence of fractures in most of the studied grains.

All the data from the in situ ablation of large (>50 μm diameter) zoned zircon grains plot to the right of the concordia (Table 3; Fig. 4) line, because of the presence of either common Pb in these grains or recent Pb-loss. It is noteworthy to add that the data plot as a group in each sample, with upper intercepts of ca. 420 Ma in WX86NB-262, ca. 410 Ma in WX86NB-254, and ca. 401 Ma in WX86NB-240. Common-Pb corrected data for four near-concordant analyses yield an overlapping concordia age of 420.0 ± 5.4 Ma (MSWD = 0.20, probability of concordance = 0.65) for sample WX86NB-262; 410.2 ± 4.7 Ma (MSWD = 0.37, probability of concordance

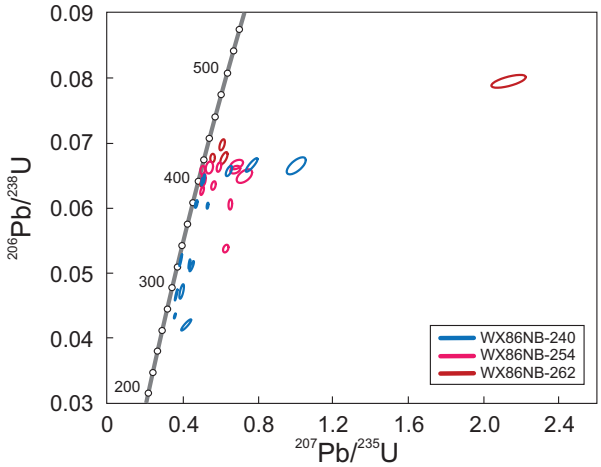

Figure 4. A Part of the concordia line for in situ zircon study showing that zircon grains plot to the right of the concordia.

Table 3. Laser ablation ICP-MS data for in situ zircon grains from two units of the SNRPS.

Spot name		Isotope ratios										Ages (Ma)				
		^{232}Th (ppm)	^{238}U (ppm)	U/Th	$^{206}Pb/^{204}Pb$	†%Pb*	$^{207}Pb/^{235}U$	2σ	$^{206}Pb/^{238}U$	2σ	err. corr.	$^{207}Pb/^{235}U$	2σ	$^{206}Pb/^{238}U$	2σ	%conc
Mount Elizabeth Granite (Sample WX86NB-240 UTM: E=688520, N=5241600, Zone 19T)																
Z-240-G3-1		6290	14630	2.326	2135	98.89	0.36	0.00	0.0434	0.0003	0.72	313	9	274	6	87.5
Z-240-G3-2		3582	11000	3.071	1861	98.76	0.44	0.01	0.0514	0.0006	0.72	368	10	323	8	87.7
Z-240-G3-3		7440	17870	2.402	1506	98.61	0.45	0.01	0.0511	0.0007	0.82	375	11	321	8	85.6
Z-240-G4-1	*	1238	2678	2.163	5877	99.66	0.47	0.01	0.0606	0.0005	0.58	394	11	379	8	96.3
Z-240-G4-2	*	1497	3319	2.217	7826	99.71	0.50	0.01	0.0640	0.0005	0.53	415	11	400	9	96.4
Z-240-G5-1	*	1576	3970	2.519	9074	99.66	0.51	0.01	0.0645	0.0005	0.68	421	11	404	9	95.9
Z-240-G5-2		2700	4080	1.511	1995	98.77	0.53	0.00	0.0604	0.0004	0.43	435	11	378	8	87.0
Z-240-G9-1		1094	18550	16.956	776	97.51	0.42	0.02	0.0420	0.0007	0.91	349	16	265	7	76.0
Z-240-G9-2	*	573	13160	22.967	4227	99.42	0.37	0.01	0.0467	0.0007	0.91	316	9	294	7	93.0
Z-240-G12-1		1890	6080	3.217	306	93.36	1.01	0.04	0.0665	0.0011	0.67	705	26	415	11	58.9
Z-240-G15-1	*	3036	30200	9.947	15962	99.81	0.39	0.01	0.0520	0.0008	0.92	335	10	327	8	97.7
Z-240-G15-2		5590	14760	2.640	1718	98.78	0.40	0.01	0.0471	0.0009	0.68	337	12	297	8	88.0
Z-240-G16-1		864	2041	2.362	614	96.45	0.77	0.02	0.0666	0.0008	0.88	576	19	416	10	72.2
Z-240-G16-2		1870	3163	1.691	1019	97.93	0.65	0.01	0.0657	0.0007	0.65	507	14	410	9	80.9
Mount LaTour Granite (Sample WX86NB-254 UTM: E = 685440, N = 5247810, Zone 19T)																
Z-254-G2-1		513	1374	2.678	466	95.96	0.63	0.01	0.0537	0.0005	0.36	496	14	337	7	68.1
Z-254-G4-1		764	1947	2.548	665	96.89	0.66	0.01	0.0605	0.0006	0.15	512	14	379	8	73.9
Z-254-G5-1		342	722	2.115	1915	98.74	0.56	0.01	0.0635	0.0006	0.38	453	13	397	9	87.5
Z-254-G6-1	*	452	1111	2.459	2293	99.50	0.54	0.02	0.0662	0.0008	0.21	441	14	413	9	93.8
Z-254-G6-2		310	988	3.191	747	97.42	0.68	0.02	0.0659	0.0005	0.36	526	17	411	9	78.2
Z-254-G6-3	*	351	893	2.546	5108	99.84	0.51	0.01	0.0658	0.0006	0.20	416	12	411	9	98.7
Z-254-G6-4		438	1062	2.425	832	97.56	0.69	0.03	0.0667	0.0005	0.43	529	21	416	9	78.7
Z-254-G8-1	*	230	760	3.307	3277	99.67	0.51	0.01	0.0644	0.0007	0.23	420	13	402	9	95.8
Z-254-G8-2		538	2338	4.346	616	96.64	0.73	0.03	0.0649	0.0009	0.53	556	23	405	10	72.9
Z-254-G9-1	*	593	1526	2.572	1529	98.76	0.59	0.01	0.0663	0.0006	0.41	474	13	414	9	87.4
Z-254-G10-1	*	964	2062	2.139	5975	99.49	0.51	0.01	0.0627	0.0005	0.56	415	11	392	8	94.5
Mount LaTour Granite (Sample WX86NB-262 UTM: E = 681360, N = 5247860, Zone 19T)																
Z-262-G2-1	*	399	716	1.794	1519	99.00	0.61	0.01	0.0697	0.0007	0.52	483	14	435	10	89.9
Z-262-G2-2		452	819	1.813	109	82.72	2.13	0.08	0.0794	0.0008	0.67	1154	32	493	11	42.7
Z-262-G3-1	*	1070	2051	1.917	5897	99.73	0.50	0.01	0.0637	0.0003	0.28	411	11	398	8	96.9
Z-262-G4-1	*	513	1165	2.271	2772	99.37	0.56	0.01	0.0677	0.0005	0.11	451	13	422	9	93.6
Z-262-G4-2	*	701	1397	1.994	1422	98.62	0.62	0.02	0.0676	0.0008	0.67	490	16	422	10	86.1

Table 3. Continued.

Spot name	Isotope ratios										Ages (Ma)				
	^{232}Th (ppm)	^{238}U (ppm)	U/Th	^{206}Pb/^{204}Pb	†%Pb*	^{207}Pb/^{235}U	2σ	^{206}Pb/^{238}U	2σ	err. corr.	^{207}Pb/^{235}U	2σ	^{206}Pb/^{238}U	2σ	%conc
Plesovice zircon standard															
Plesovice-6	117	917	7.813	5990	99.72	0.41	0.01	0.0538	0.0006	0.20	347	11	338	8	97.2
Plesovice-5	30	394	12.955	2291	99.86	0.39	0.01	0.0542	0.0006	0.17	337	12	340	8	101.1
Plesovice-4	39	471	12.167	2216	99.83	0.40	0.01	0.0539	0.0006	0.08	340	11	339	8	99.4
Plesovice-3	36	461	12.841	-13380	99.86	0.39	0.01	0.0541	0.0004	0.20	339	12	339	7	100.2
Plesovice-2	108	938	8.665	2311	99.82	0.40	0.01	0.0539	0.0004	0.35	340	11	339	7	99.6
Plesovice-1	58	631	10.943	1114	99.79	0.40	0.01	0.0538	0.0005	0.24	341	11	338	8	99.1

* = used for concordia and weighted mean ^{206}Pb/^{238}U calculations; † = estimated from Andersen (2002) method; Pb* = Radiogenic Pb.

= 0.54) for sample WX86NB-254; and 401.7 ± 4.3 Ma (MSWD = 7.2, probability of concordance = 0.007) for sample WX86NB-240. The slightly older age of 420.0 ± 5.4 Ma in WX86NB-262 may be due to inadvertent ablation of inherited zircon cores in this sample. Samples WX86NB-240 and -254 show more evidence of recent Pb-loss. It is important to note that given the very small ^{204}Pb signals and potential for minor inheritance, the common-Pb corrected in situ U-Pb zircon data are considered a less reliable estimate for crystallization ages compared to the monazite results.

The ablation of ninety-eight mounted zircon grains from the Mount Elizabeth Granite yielded nine near-concordant spots overlapping within uncertainty, resulting in a concordia age of 417.5 ± 1.6 Ma (MSWD = 1.2, probability of concordance = 0.27; Table 4; Fig. 5a), and a weighted

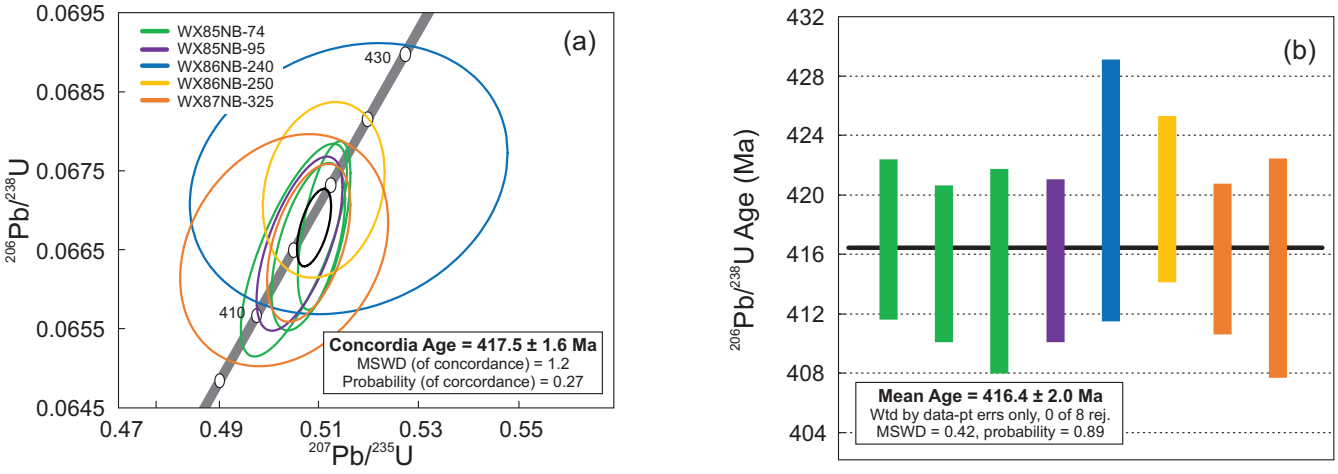

Figure 5. (a) Concordia plot for laser ablation ICP-MS analyses of separated zircon (unpolished run) grains from the seven samples of the Mount Elizabeth Granite (b) Plot of weighted mean of ^{206}Pb/^{238}U ages for zircon grains of the same samples. Error ellipses, and box heights are at the 2σ level.

Table 4. Laser ablation ICP-MS data for separated zircon grains (unpolished run) from the Mount Elizabeth Granite of SNRPS.

Spot name		Isotope ratios										Ages (Ma)				
		^{232}Th (ppm)	^{238}U (ppm)	U/Th	^{206}Pb/^{204}Pb	†%Pb*	^{207}Pb/^{235}U	2σ	^{206}Pb/^{238}U	2σ	err. corr.	^{207}Pb/^{235}U	2σ	^{206}Pb/^{238}U	2σ	%conc
(Sample WX85NB-74 UTM: E = 689260, N = 5247690, Zone 19T)																
74-1-1		8180	1425	5.74	7100	99.80	0.489	0.011	0.063	0.001	0.804	404	7	396	8	102.0
74-3-1		5520	1359	4.06	1150	98.39	0.439	0.012	0.058	0.002	0.393	369	10	365	9	101.1
74-3-2	*	5453	1216	4.48	13321	99.85	0.511	0.004	0.067	0.001	0.605	419	3	417	5	100.5
74-5-1	*	5810	990	5.87	10923	99.92	0.508	0.006	0.067	0.001	0.559	417	4	415	5	100.4
74-5-2		7400	2502	2.96	8412	99.78	0.474	0.007	0.061	0.001	0.883	393	5	380	7	103.4
74-6-1		7010	1672	4.19	41460	99.98	0.569	0.009	0.074	0.001	0.540	457	6	458	8	99.7
74-6-2	*	8250	1332	6.19	3608	99.91	0.505	0.009	0.067	0.001	0.743	415	6	415	7	100.0
74-7-1		183.9	59.72	3.08	546	99.78	0.648	0.023	0.082	0.001	0.299	506	15	508	8	99.6
74-7-2		124.6	59	2.11	1095	99.77	0.656	0.027	0.083	0.001	0.280	512	16	513	9	99.8

Table 4. Continued.

Spot name		Isotope ratios										Ages (Ma)				
		^{232}Th (ppm)	^{238}U (ppm)	U/Th	^{206}Pb/ ^{204}Pb	†%Pb*	^{207}Pb/ ^{235}U	2σ	^{206}Pb/ ^{238}U	2σ	err. corr.	^{207}Pb/ ^{235}U	2σ	^{206}Pb/ ^{238}U	2σ	%conc
(Sample WX85NB-74 continued)																
74-8-1		7690	510.7	15.06	2110	99.35	0.711	0.014	0.082	0.001	0.704	547	8	511	7	107.1
74-8-2		8170	694	11.77	7232	99.75	0.572	0.010	0.072	0.001	0.655	459	6	447	5	102.8
74-9-1		4320	1256	3.44	1953	99.08	0.582	0.009	0.067	0.001	0.667	465	6	420	6	110.9
74-9-2		3608	994	3.63	9147	99.77	0.529	0.006	0.067	0.001	0.522	431	4	421	5	102.5
74-10-1		3358	748	4.49	834	97.22	0.687	0.016	0.066	0.001	0.392	531	10	410	6	129.4
74-10-2		3046	694	4.39	4719	99.42	0.556	0.008	0.067	0.001	0.454	449	5	420	5	106.9
74-11-1		5490	1149	4.78	1620	99.05	0.569	0.017	0.075	0.001	0.620	459	10	465	6	98.6
74-11-2		5240	1041	5.03	4039	99.64	0.552	0.011	0.069	0.001	0.568	446	7	427	7	104.4
74-12-1		4970	990	5.02	32571	99.56	0.539	0.015	0.067	0.002	0.418	438	9	418	11	104.6
74-12-2		7690	1750	4.39	6017	99.72	0.529	0.009	0.067	0.001	0.674	431	6	418	8	103.1
(Sample WX85NB-80 UTM: E = 690660, N = 5242780, Zone 19T)																
80-13-1		4960	371	13.37	1029	98.42	0.537	0.022	0.072	0.001	0.484	435	12	448	6	97.1
80-14-1		5760	576	10.00	1993	99.22	0.653	0.009	0.076	0.001	0.417	510	5	472	8	108.1
80-16-1		4827	603	8.00	3161	99.40	0.551	0.008	0.067	0.001	0.682	446	5	415	7	107.4
80-20-1		6950	1393	4.99	3226	99.98	0.652	0.027	0.083	0.001	0.745	510	13	513	8	99.3
80-23-1		3472	418.2	8.30	10350	99.73	0.614	0.007	0.075	0.001	0.329	487	4	468	7	103.9
80-25-1		4850	529	9.17	1433	98.78	0.590	0.017	0.076	0.002	0.589	474	11	470	9	100.8
80-26-1		4590	410	11.20	21000	99.65	0.547	0.006	0.068	0.001	0.569	443	4	424	6	104.5
80-27-1		5123	490	10.46	3759	99.26	0.562	0.008	0.067	0.001	0.688	453	5	419	7	107.9
(Sample WX85NB-81 UTM: E = 690590, N = 5245630, Zone 19T)																
81-1-1		1780	398	4.47	8345	99.93	0.504	0.041	0.067	0.004	0.510	414	25	415	21	99.8
81-3-1		11530	1261	9.14	2389	99.37	0.644	0.010	0.076	0.001	0.644	505	6	471	7	107.2
81-6-1		4581	336.3	13.62	34540	100.00	0.571	0.005	0.075	0.001	0.430	459	3	463	6	99.0
(Sample WX85NB-95 UTM: E = 688910, N = 5239180, Zone 19T)																
95-1-1		3078	745	4.13	19833	99.83	0.563	0.007	0.072	0.001	0.629	453	5	447	6	101.5
95-10-1		3070	727	4.22	1640	99.17	0.564	0.012	0.066	0.001	0.446	454	7	411	5	110.6
95-11-1		3610	700	5.16	2618	99.64	0.617	0.009	0.076	0.001	0.470	487	6	469	7	103.8
95-12-1	*	4230	1007	4.20	28743	99.96	0.506	0.007	0.067	0.001	0.641	416	5	416	5	100.0
95-13-1		2530	577	4.38	6163	99.97	0.579	0.009	0.075	0.001	0.684	463	6	468	7	99.1
95-14-1		2050	429	4.78	2461	98.80	0.611	0.018	0.069	0.001	0.690	484	11	430	6	112.6
95-15-1		4330	756	5.73	382	95.57	0.571	0.027	0.075	0.001	0.376	455	17	467	7	97.3
95-16-1		4210	1083	3.89	4897	99.64	0.538	0.009	0.067	0.001	0.554	437	6	416	6	104.9
95-17-1		4236	1082	3.91	4115	99.76	0.598	0.008	0.075	0.001	0.615	476	5	464	8	102.5
95-18-1		5380	1481	3.63	7990	99.78	0.551	0.010	0.070	0.001	0.153	445	6	433	8	102.8
95-19-1		6180	119.7	51.63	1593	98.87	0.593	0.009	0.068	0.001	0.082	472	6	421	7	112.2
95-2-1		7900	1381	5.72	4603	99.94	0.613	0.007	0.079	0.001	0.545	485	4	489	8	99.3
95-20-1		2810	537	5.23	21333	99.88	0.547	0.006	0.070	0.001	0.417	443	4	438	5	101.1
95-21-1		7750	1662	4.66	2682	99.29	0.642	0.012	0.076	0.002	0.432	503	8	469	10	107.3
95-23-1		5510	468	11.77	2207	99.20	0.571	0.011	0.067	0.001	0.681	458	7	420	7	109.2
95-24-1		6730	1590	4.23	1138	98.45	0.606	0.013	0.065	0.001	0.144	484	8	408	8	118.6
95-25-1		8990	2350	3.83	1270	98.74	0.353	0.023	0.042	0.002	0.828	307	15	264	10	116.1
95-3-1		4170	1050	3.97	13473	99.99	0.579	0.007	0.075	0.001	0.405	464	4	466	6	99.6
95-4-1		8160	1100	7.42	7820	99.86	0.529	0.009	0.068	0.001	0.498	431	6	427	8	101.0
95-5-1		7300	524	13.93	22667	99.96	0.548	0.007	0.072	0.001	0.558	444	5	445	8	99.6
95-6-1		11730	4640	2.53	799	98.05	0.372	0.017	0.053	0.001	0.323	321	10	335	8	95.9
95-7-1		5160	848	6.08	4037	99.86	0.593	0.009	0.075	0.001	0.684	472	6	467	7	101.2
95-8-1		2810	631	4.45	3324	99.42	0.571	0.012	0.069	0.001	0.497	458	8	430	7	106.5
95-9-1		8730	3100	2.82	2309	99.17	0.579	0.008	0.068	0.001	0.496	464	5	422	6	109.9

Table 4. Continued.

Spot name		Isotope ratios										Ages (Ma)				
		^{232}Th (ppm)	^{238}U (ppm)	U/Th	^{206}Pb/^{204}Pb	†%Pb*	^{207}Pb/^{235}U	2σ	^{206}Pb/^{238}U	2σ	err. corr.	^{207}Pb/^{235}U	2σ	^{206}Pb/^{238}U	2σ	%conc
(Sample WX86NB-240 UTM: E=688520, N=5241600, Zone 19T)																
240-1-1		11800	2650	4.45	713	97.19	0.524	0.018	0.067	0.001	0.071	427	7	417	7	102.3
240-1-2		8680	2058	4.22	4176	99.53	0.577	0.015	0.071	0.001	0.749	463	9	440	6	105.3
240-2-1		5278	1530	3.45	4285	99.59	0.622	0.007	0.076	0.001	0.317	491	5	470	6	104.5
240-3-1		9940	1817	5.47	2355	99.26	0.526	0.012	0.070	0.001	0.348	429	7	434	5	98.8
240-3-2		9540	1884	5.06	5813	99.65	0.575	0.010	0.071	0.001	0.462	462	6	442	5	104.4
240-8-1		5820	1742	3.34	17336	99.85	0.577	0.020	0.073	0.001	0.040	462	12	455	7	101.7
240-8-2	*	8650	2594	3.33	1336	98.61	0.516	0.026	0.067	0.001	0.190	422	10	420	9	100.4
240-9-1		2960	409	7.24	1903	99.16	0.523	0.017	0.068	0.001	0.036	426	9	426	5	100.1
240-9-2		5030	1293	3.89	3327	99.49	0.591	0.046	0.072	0.001	0.407	471	25	446	5	105.7
(Sample WX86NB-250 UTM: E = 685360, N = 5254810, Zone 19T)																
250-1-1		850	310	2.74	2006	99.11	0.631	0.023	0.072	0.001	0.434	496	13	446	6	111.0
250-2-1		2430	528	4.60	2500	99.73	0.451	0.008	0.059	0.001	0.565	378	6	367	6	102.8
250-3-1		732	219.2	3.34	2089	99.84	0.554	0.013	0.071	0.001	0.344	448	8	445	6	100.6
250-4-1	*	691	438	1.58	-8288	99.85	0.511	0.010	0.067	0.001	0.193	420	7	420	6	100.1
250-5-1		1030	596.9	1.73	1386	99.83	0.551	0.017	0.071	0.001	0.037	445	11	443	5	100.6
250-6-1		1970	625	3.15	3032	99.72	0.572	0.012	0.071	0.001	0.387	459	8	445	5	103.2
250-7-1		2678	2427	1.10	129	85.43	0.549	0.091	0.063	0.001	0.597	429	33	395	8	108.7
250-8-1		3750	1903	1.97	1229	99.00	0.690	0.021	0.078	0.001	0.618	532	12	482	8	110.3
250-9-1		1540	656	2.35	7045	99.94	0.547	0.009	0.071	0.001	0.526	443	6	444	6	99.7
(Sample WX87NB-325 UTM: E = 684600, N = 5236150, Zone 19T)																
325-1-1		4268	1566	2.73	634	97.55	0.493	0.036	0.068	0.002	0.577	407	16	425	11	95.8
325-10-1		804	263	3.06	308	94.64	0.454	0.064	0.064	0.001	0.650	365	43	402	8	90.7
325-11-1		786.4	503.3	1.56	2292	99.25	0.545	0.011	0.065	0.001	0.168	442	7	406	7	108.8
325-12-1		5320	1986	2.68	663	97.38	0.355	0.020	0.050	0.002	0.499	307	15	312	12	98.4
325-13-1		1887	574	3.29	3515	99.70	0.532	0.010	0.067	0.001	0.431	433	7	421	5	102.8
325-14-1	*	2118	540	3.92	5068	100.02	0.508	0.007	0.067	0.001	0.478	417	5	416	5	100.3
325-15-1		1742	594.9	2.93	567	97.09	0.456	0.032	0.063	0.002	0.304	381	21	391	11	97.4
325-16-1		1391	364	3.82	746	97.37	0.558	0.037	0.071	0.001	0.345	449	22	440	6	102.2
325-17-1	*	11750	2967	3.96	815	97.90	0.503	0.017	0.067	0.001	0.241	413	12	415	7	99.5
325-18-1		562	245.2	2.29	791	98.96	0.592	0.031	0.068	0.001	0.140	471	18	421	6	111.9
325-19-1		952	374.5	2.54	1738	99.88	0.604	0.021	0.075	0.001	0.343	479	13	465	5	103.0
325-2-1		1258	375.3	3.35	1007	98.49	0.624	0.014	0.068	0.002	0.718	492	9	422	11	116.6
325-20-1		19180	2530	7.58	3779	99.77	0.365	0.010	0.053	0.002	0.779	315	9	332	11	94.9
325-3-1		1730	768	2.25	481	96.98	0.471	0.037	0.070	0.001	0.330	394	24	439	6	89.7
325-4-1		5650	2270	2.49	3339	99.67	0.505	0.006	0.064	0.001	0.633	415	4	400	7	103.5
325-5-1		4290	1681	2.55	4521	99.67	0.546	0.008	0.068	0.001	0.483	442	5	424	6	104.2
325-6-1		1330	414	3.21	1524	98.90	0.665	0.035	0.074	0.001	0.179	518	19	463	6	111.9
325-7-1		2817	873	3.23	1773	98.93	0.611	0.008	0.069	0.001	0.200	484	5	432	5	111.9
325-8-1		1704	575	2.96	2042	98.75	0.621	0.012	0.068	0.001	0.015	491	7	421	6	116.5
325-9-1		1067	237.8	4.49	1567	98.12	0.692	0.012	0.070	0.001	0.674	533	8	439	6	121.6
Plesovice zircon standard																
Plesovice-1		937.1	83.04	11.28	8922	99.92	0.392	0.006	0.054	0.001	0.199	336	5	337	4	99.6
Plesovice-2		890.2	77.57	11.48	4259	99.88	0.389	0.006	0.053	0.001	0.107	334	5	335	4	99.5
Plesovice-3		633.8	66.08	9.59	2679	99.94	0.387	0.006	0.054	0.001	0.094	333	4	336	4	98.9
Plesovice-4		634.7	53.84	11.79	2403	99.92	0.392	0.008	0.054	0.001	0.086	335	6	338	4	99.2
Plesovice-5		636.7	68.18	9.34	100	99.85	0.393	0.007	0.053	0.001	0.020	336	5	335	5	100.3
Plesovice-6		599.3	56.63	10.58	-11557	99.72	0.400	0.010	0.054	0.001	0.191	342	7	337	4	101.5
Plesovice-7		564.5	52.46	10.76	2101	99.81	0.395	0.010	0.054	0.001	0.232	338	7	336	4	100.4

* = used for concordia and weighted mean ^{206}Pb/^{238}U calculations; † = estimated from Andersen (2002) method; Pb* = Radiogenic Pb.

average $^{206}Pb/^{238}U$ age of 416.4 ± 2.0 Ma (MSWD = 0.42, probability of concordance = 0.89; Fig. 5b). The same grains were ablated once more after polishing the epoxy, yielding a concordia age of 417.5 ± 1.9 Ma (MSWD = 1.3, probability of concordance = 0.26; Table 5; Fig. 6a); the weighted average $^{206}Pb/^{238}U$ age is calculated to be 418.6 ± 2.6 Ma (MSWD = 1.18, probability of concordance = 0.31; Fig. 6b). The weighted average of both runs in stage two are in agreement; however, the amount of correction is less in the polished run. As a result, the weighted average of this run is believed to represent the best crystallization age of Mount Elizabeth Granite. This age is in a complete agreement with the results of the monazite study, and may confirm the accuracy of the result. Based on the overlap between the 2σ error envelopes for the results of in situ monazite study, and separated monazite and zircon grains, we assigned an average age of 417.3 ± 0.96 Ma (95% confident) as the best estimate of crystallization age for Mount Elizabeth Granite.

Results of this study clearly showed inheritance signatures in zircon grains in the seven mineral-separate samples, including WX86NB-240, examined in the stage two analyses. It is especially an issue in unpolished grain mounts, in which the probably density plot shows peaks at

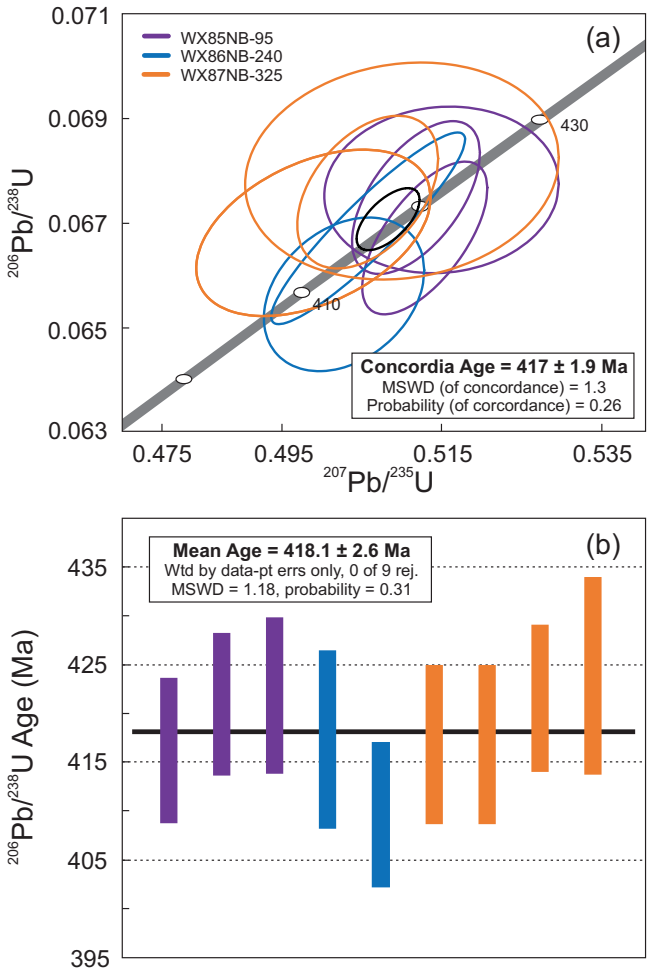

Figure 6. (a) Concordia plot for laser ablation ICP-MS analyses of separated zircon (polished run) grains from the seven samples of the Mount Elizabeth Granite. (b) Plot of weighted mean of $^{206}Pb/^{238}U$ ages for zircon grains of the same samples. Error ellipses, and box heights are at the 2σ sigma level.

Table 5. Laser ablation ICP-MS data for separated zircon grains (polished run) from the Mount Elizabeth Granite of SNRPS.

Spot name		Isotope ratios										Ages (Ma)				
		^{232}Th (ppm)	^{238}U (ppm)	U/Th	$^{206}Pb/^{204}Pb$	†%Pb*	$^{207}Pb/^{235}U$	2σ	$^{206}Pb/^{238}U$	2σ	err. corr.	$^{207}Pb/^{235}U$	2σ	$^{206}Pb/^{238}U$	2σ	%conc
(Sample WX85NB-74 UTM: E = 689260, N = 5247690, Zone 19T)																
74-z1-1		2	40	21.838	2041	99.78	0.67	0.06	0.0851	0.0034	0.08	520	38	526	20	101.2
74-z1-2		2	45	20.229	211	98.68	0.72	0.06	0.0809	0.0026	0.02	554	35	501	16	90.4
74-z1-3		3	52	19.900		99.40	0.70	0.05	0.0820	0.0024	0.15	538	29	508	14	94.4
(SampleWX85NB-80UTM:E=690660,N=5242780,Zone19T)																
80-z1-1		16	436	27.070	6659	99.84	0.45	0.01	0.0600	0.0010	0.24	377	8	376	8	99.6
80-z2-1		50	1284	25.580		99.91	0.50	0.01	0.0650	0.0010	0.40	410	6	408	7	99.6
(SampleWX85NB-81UTM:E=690590,N=5245630,Zone19T)																
81-z1-1		10	240	23.952	-38200	99.88	0.48	0.01	0.0627	0.0011	0.39	400	4	392	7	98.1
81-z1-2		13	323	23.944	19860	99.82	0.48	0.01	0.0627	0.0011	0.39	401	5	392	7	97.8
(SampleWX85NB-95UTM:E=688910,N=5239180,Zone19T)																
95-z1-1	*	101	2461	24.439	14992	99.90	0.51	0.01	0.0667	0.0012	0.65	420	4	416	7	99.0
95-z1-2	*	144	3649	25.340	128650	99.99	0.51	0.01	0.0675	0.0012	0.58	420	4	421	7	100.4
95-z2-1		91	1856	20.418	1061	97.88	0.52	0.03	0.0657	0.0014	0.51	426	77	83	410	19.5
95-z2-2		194	4970	25.566	16411	99.79	0.48	0.01	0.0638	0.0012	0.95	398	3	399	7	100.3
95-z3-1	*	22	553	24.688	-3188	99.84	0.52	0.01	0.0676	0.0013	0.07	422	8	422	8	99.9
95-z4-1		166	3700	22.303	30350	99.96	0.55	0.01	0.0712	0.0013	0.52	443	4	443	8	100.0

Table 5. Continued.

Spot name		Isotope ratios										Ages (Ma)				
		^{232}Th (ppm)	^{238}U (ppm)	U/Th	^{206}Pb/^{204}Pb	†%Pb*	^{207}Pb/^{235}U	2σ	^{206}Pb/^{238}U	2σ	err. corr.	^{207}Pb/^{235}U	2σ	^{206}Pb/^{238}U	2σ	%conc
(SampleWX86NB-240UTM:E=688520,N=5241600,Zone19T)																
240-z1-1	*	52	1319	25.268	4305	99.70	0.51	0.01	0.0669	0.0015	0.92	415	7	417	9	100.5
240-z1-2	*	51	1309	25.921	8470	99.94	0.50	0.01	0.0656	0.0012	0.31	413	6	410	7	99.1
240-z1-3		83	1976	23.693	5115	99.69	0.52	0.01	0.0683	0.0014	0.93	425	6	426	9	100.3
240-z2-1		270	5330	19.741	1003	98.09	0.49	0.01	0.0641	0.0012	0.38	403	38	47	401	11.7
(SampleWX86NB-250UTM:E=685360,N=5254810,Zone19T)																
250-z1-1		1	19	15.254		98.93	1.00	0.05	0.1074	0.0028	0.14	700	27	658	16	94.0
250-z1-2		6	55	9.901	702	99.44	1.79	0.10	0.1729	0.0043	0.21	1030	37	1028	24	99.8
250-z2-1		61	1437	23.596	-9652	99.99	0.53	0.01	0.0699	0.0013	0.32	428	7	436	8	101.8
250-z2-2		32	803	24.784	962	98.86	0.51	0.01	0.0673	0.0015	1.00	420	6	420	9	99.8
250-z3-1		27	634	23.604	1449	99.58	0.50	0.01	0.0671	0.0014	0.45	409	5	419	8	102.4
250-z4-1		56	1463	25.940	1307	98.69	0.43	0.01	0.0583	0.0012	1.00	366	4	365	7	99.8
(SampleWX87NB-325UTM:E=684600,N=5236150,Zone19T)																
325-z1-1		7	171	26.098	1938	99.76	0.52	0.02	0.0692	0.0015	0.06	425	16	431	9	101.4
325-z2-1	*	34	907	26.944	25033	99.98	0.50	0.01	0.0668	0.0013	0.42	412	9	417	8	101.1
325-z3-1		21	447	21.079	2986	99.25	0.57	0.02	0.0671	0.0014	0.24	454	9	419	9	92.2
325-z4-1	*	34	908	26.944	25033	99.98	0.50	0.01	0.0668	0.0013	0.42	412	9	417	8	101.1
325-z5-1	*	37	969	25.979	3490	99.90	0.51	0.01	0.0676	0.0012	0.43	415	5	422	7	101.5
325-z5-2		5	141	26.844	-3307	99.58	0.53	0.02	0.0676	0.0015	0.09	430	15	421	9	98.0
325-z6-1		23	383	16.428	654	97.76	0.54	0.01	0.0706	0.0015	1.00	441	5	439	9	99.6
325-z7-1		10	277	28.304	-4835	99.91	0.51	0.02	0.0679	0.0014	0.03	415	14	423	8	102.0
325-z8-1	*	9	226	25.929	2918	99.89	0.51	0.02	0.0680	0.0017	0.12	418	11	424	10	101.4
Plesovice zircon standard																
Plesovice-1		2	60	31.354	3880	99.85	0.40	0.01	0.0541	0.0011	0.18	343	9	340	7	99.0
Plesovice-2		3	82	31.212	568	99.87	0.39	0.01	0.0540	0.0013	0.49	334	8	339	8	101.3
Plesovice-3		3	87	32.434	1129	99.96	0.39	0.01	0.0533	0.0011	0.48	332	6	335	7	100.9
Plesovice-4		2	67	34.462	2088	99.77	0.39	0.01	0.0536	0.0013	0.16	336	9	337	8	100.1
Plesovice-5		2	60	31.702	-946	99.79	0.40	0.01	0.0540	0.0011	0.14	338	10	339	7	100.3
Plesovice-6		1	38	33.421	824	99.64	0.42	0.02	0.0530	0.0014	0.30	352	13	333	8	94.6
Plesovice-7		8	268	35.536	-5182	99.96	0.40	0.01	0.0543	0.0010	0.37	340	6	341	6	100.2
Plesovice-8		9	313	33.991	-19263	99.78	0.40	0.01	0.0538	0.0012	0.60	341	7	338	8	99.2
Plesovice-9		9	282	31.939	3440	99.82	0.39	0.01	0.0542	0.0011	0.48	337	5	340	7	100.8
Plesovice-10		8	262	33.886	2117	99.89	0.39	0.01	0.0541	0.0011	0.61	337	6	341	7	101.1

* = used for concordia and weighted mean ^{206}Pb/^{238}U calculations; † = estimated from Andersen (2002) method; Pb* = radiogenic Pb.

ca. 444 Ma, 465 Ma, and 512 Ma (Fig. 7). The polished grain mounts also encountered inheritance at ca. 500 Ma (Table 5), as well as some cores with Grenvillian ages (ca. 1000 Ma). Interestingly, the zircon grain with the Grenvillian core has one of the lowest U contents among the studied grains (U <55 ppm). Inherited zircon is common in magmatic rocks, especially in peraluminous or S-type granites (Harrison *et al.* 1987). Zircon solubility is directly related to temperature (i.e., the solubility increases in less evolved systems having higher temperatures), and to a lesser extent depends on magma composition (e.g., the cation ratio (Na + K + 2Ca) / (Al + Si), Watson and Harrison (1983)). As a result, inherited zircon was expected in samples of the peraluminous Mount Elizabeth Granite. In order to further study the possibility of inheritance in zircon grains, the zircon saturation temperature was calculated using the empirical model of Watson and Harrison (1983), and the whole-rock chemical data available from Whalen (1993). The temperatures were estimated to vary from 830 to 839 °C in the Mount Elizabeth Granite, and from 833 to 824 °C in the Mount LaTour Granite. These temperatures are higher than the common normal magma temperatures for granitoid rocks of this composition (maximum of 740 to 762 °C; Chappell *et al.* 1998). The presence of inherited zircon, and/or other zirconium-bearing minerals would result in a higher calculated temperature (Yang 2005); therefore, the calculated zircon saturation temperatures are assumed to represent the maximum temperatures.

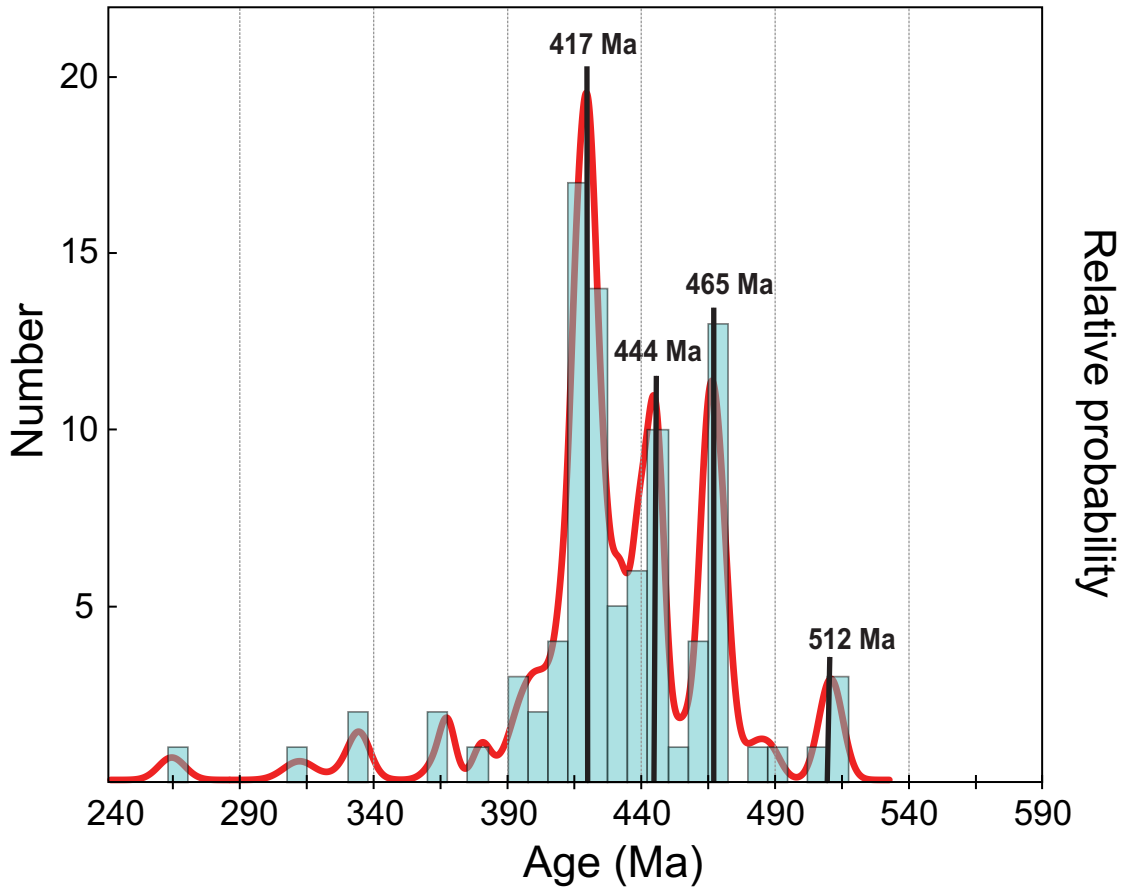

Figure 7. Probability density plot for the unpolished grain mounts shows peaks at ca. 444 Ma, 465 Ma, and 512 Ma indicating inheritance in the examined zircons.

Inheritance is commonly an issue in peraluminous magmas (Klötzli *et al.* 2001) due to the lower zircon solubility in magmas of this composition (Watson and Harrison 1983). Previous studies of zircon grains in New Brunswick granitoid rocks (Bevier and Whalen 1990; Roddick and Bevier 1995) indicated significant inheritance. Whalen (1993) reported an upper intercept of about 1.4 Ga for several Ordovician granites in the Gander zone. Roddick and Bevier (1995) also documented Grenvillian xenocrystic zircons in the Meridian Brook and Pabineau Falls granites in northeastern New Brunswick. Furthermore, both zircon populations in sediments and inherited grains in granites contain a predominance of 1.5 ± 0.2 Ga grains in the Gander Zone in Newfoundland (Whalen 1993). The Grenvillian xenocrystic cores are believed to be related to a probable Precambrian basement. Additionally, the ca. 444 Ma peak of the zircon grains represents the age of Salinic deformation and metamorphism whereas the ca. 465 Ma peak may be derived from the felsic volcanic sequence and associated intrusions related to Middle Ordovician back arc rifting (van Staal *et al.* 2009). These data suggest that Ordovician volcanic and sedimentary rocks may be the source for these granites or form a major assimilated component.

IMPLICATIONS OF THE RESULTS

Early Devonian plutonic rocks of SNRPS are not only petrographically and mineralogically similar to but also contemporaneous with the North Pole Stream granite (417 ± 1 Ma; Bevier and Whalen 1990; Whalen 1993) and Redstone Mountain Granite (419.0 ± 0.5 Ma; Wilson and Kamo 2016). All of these intrusions are medium- to coarse-grained, pink to red biotite granites crosscut by finer grained granodioritic dykes. SNRPS phases plot in an array from volcanic-arc to within-plate fields on the Rb vs. Nb + Y tectonic discrimination diagram of Pearce *et al.* (1984) and Pearce (1996) (Fig 8a), and Hf-Rb-Ta ternary diagram of Harrison *et al.* (1986) (Fig. 8b). Interestingly, all geochemical data (compiled from the study of Whalen 1993) plot in the domain of post-collisional granites defined by Pearce (1996) and S-type granitoids by Christiansen and Keith (1996) (Fig 8a). These discrimination plots purpose not only their tectonic setting, but also the protolith, melting, and crystallization histories (Christiansen and Keith 1996; Chowdhury and Lentz 2010). Samples from Mount Elizabeth Granite plot mostly in the peraluminous field, whereas the Mount LaTour samples plot in the metaluminous field of Shand (1943) (Fig. 8c).

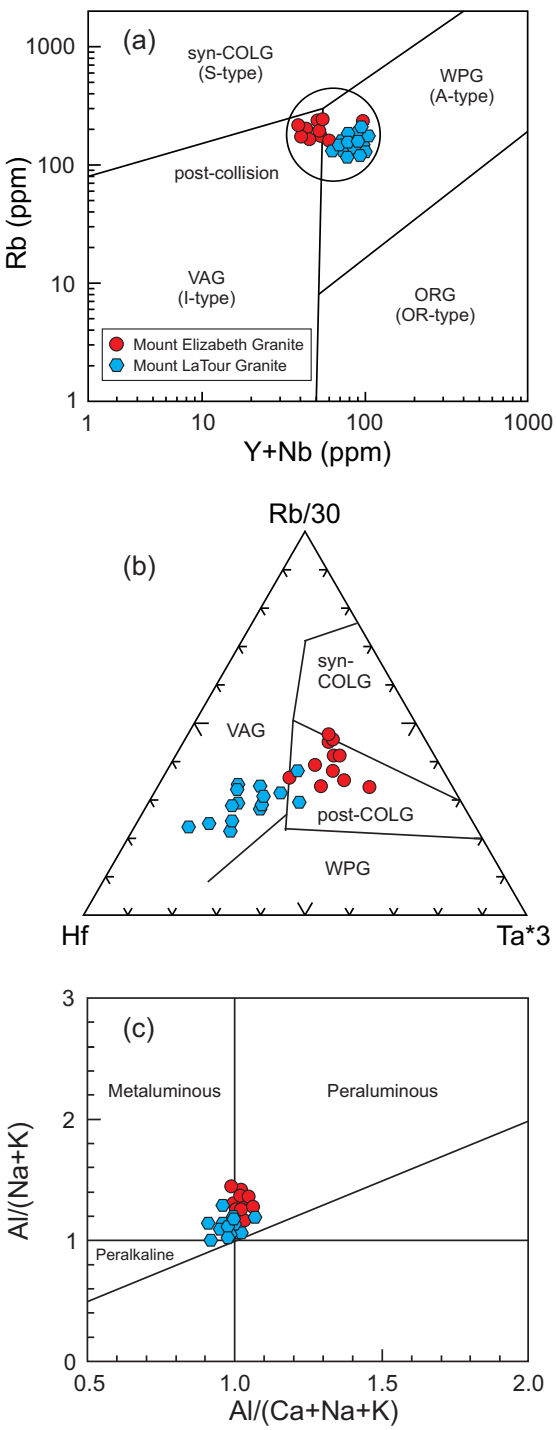

Figure 8. (a) Rb vs. Y + Nb tectonic discrimination diagram applied to the granitic samples from SNRPS (Pearce *et al.* 1984), superimposed by the post-collision granite field of Pearce (1996). Fields labelled as syn-COLG (S-type), VAG (I-type), WPG (A-type) are based on Christiansen and Keith (1996). (b) Hf-Rb-Ta tectonic discrimination diagram with fields defined by Harrison *et al.* (1986) for granites from the SNRPS. (c) Al/(Na + K) vs Al/ (Ca + Na + K) aluminum saturation index (ASI) diagram of Shand (1943) for the granites of SNRPS.

The peraluminous nature of these intrusions indicates a major supracrustal component in the source; this is supported by the close spatial relationship with the Miramichi Group, and the common presence of xenoliths of partially assimilated metasedimentary rocks in these plutons (Whalen 1993; Wilson and Kamo 2016).

Primitive mantle normalized plots could reflect tectonic affinities for felsic plutons; however, interpretation is complicated by potential fractionation of trace elements into phases such as zircon, monazite, and apatite (Whalen *et al.* 1996). Well-developed negative Ba, Sr, Eu, and Ti anomalies in both Mount Elizabeth and Mount LaTour granites may have been caused by fractionation of feldspars and oxides, respectively, although, negative Nb anomalies in these rocks (see Figs. 9a-b) probably are a source characteristic. Negative Nb anomalies are a common feature of granites derived mainly from a crustal source that in itself was derived from arc crust (Whalen *et al.* 1996; Yang *et al.* 2008).

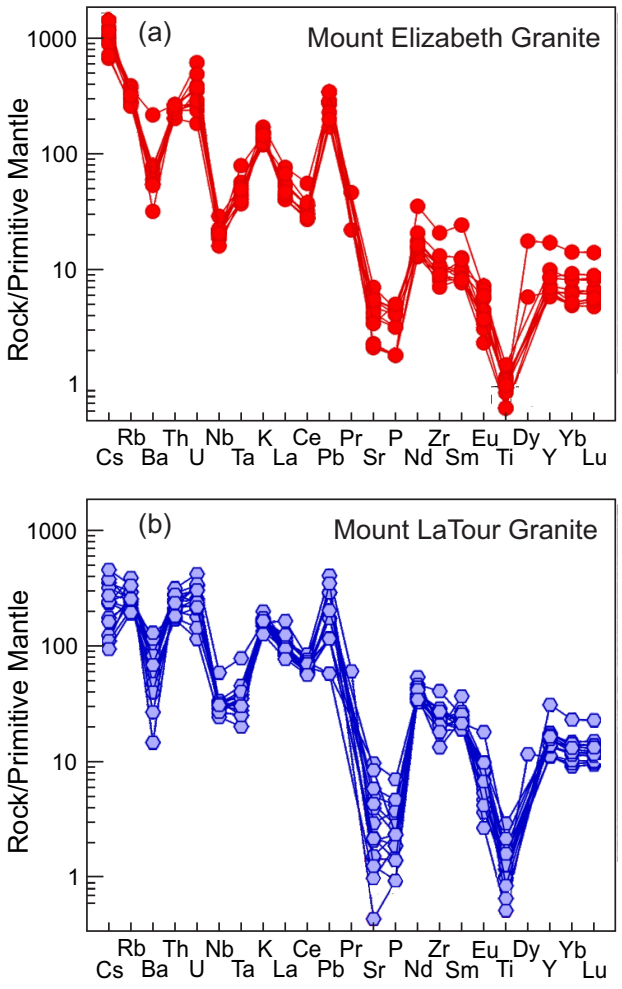

Figure 9. (a) Primitive-mantle-normalized spider diagram for Mount Elizabeth Granite, and (b) Mount LaTour Granites. Primitive mantle values are from Sun and McDonough (1989). Symbols as in Figure 8.

Whalen (1993) suggested involvement of and/or contributions from mantle-derived components for Silurian-Devonian granite magmatism of the Gander zone. Whalen *et al.* (1996) argued that these granitic intrusions were produced by partial melting of Middle Proterozoic continental basement through lithospheric delamination during Iapetus or back-arc basin closure. Rapid uplift and gravitational instability would follow either of these scenarios, which could be explained by the ca. mid-Silurian breakoff of the Tetagouche slab (Wilson and Kamo 2016). This may have caused exhumation of the Brunswick Subduction Complex and subsequent extensional collapse in the Miramichi Highlands (Wilson and Kamo 2016).

Mount Elizabeth, North Pole Stream, and Redstone granites are associated with the late Silurian magmatic phase (ca. 423 to 416 Ma) in Central New Brunswick, representatives of which are mainly exposed in the Miramichi Highlands (van Staal *et al.* 2009; Wilson and Kamo 2016). These intrusions postdate structures associated with the Salinic orogeny, and predate Acadian structures; for instance, they formed northwest of the migrating Acadian deformation front (van Staal *et al.* 2009). Furthermore, these intrusions are associated with mafic rocks that comprise up to ~ 21% of theses magmatic suites (van Staal *et al.* 2009). Van Staal *et al.* (2009) used the similarity between the spectrum and proportions of felsic and mafic phases in the SNRPS and Silurian magmatism in western and west-central Newfoundland to interpret these ca. 419–417 Ma magmatic rocks as a final, post-kinematic pulse of magmatism associated with the breakoff of the Salinic slab (Whalen *et al.* 2006; van Staal *et al.* 2009). These intrusions were further metamorphosed during the Acadian orogeny, and that could explain the common lead loss and alteration through hydrothermal activity in the examined zircon grains (van Staal *et al.* 2009; Fig. 1).

CONCLUSIONS

In situ study of monazite grains from the Mount Elizabeth and Mount LaTour granites revealed no evidence for inheritance monazite. The crystallization age is interpreted to be 417.2 ± 1.5 Ma for the Mount Elizabeth Granite and 417.7 ± 4.4 Ma for the Mount LaTour Granite which confirms the contemporaneous relationship between the felsic units of the SNRPS previously inferred by Whalen (1993). The results for monazite grains from mineral separates of the Mount Elizabeth Granite are in agreement with the dates determined by in situ analysis, with no significant effect from ^{230}Th disequilibrium.

Results of both stages of zircon studies from the Mount Elizabeth Granite showed inheritance in these grains. The Grenvillian xenocrystic cores are thought to be related to a probable Precambrian basement, whereas the ca. 444 Ma and ca. 465 Ma peaks suggest that Ordovician volcanic-sedimentary packages may have been the source of or, an assimilated component for, these granites.

The result of in situ zircon study shows evidence of advanced post-crystallization Pb-loss and common lead incorporation, and defines a younger concordia age. These results are interpreted to reflect later hydrothermal alteration and isotopic resetting rather than crystallization ages. In addition, in situ U-Pb zircon data are not reliable because of the very small ^{204}Pb signals, and do not reflect crystallization ages for these units. However, separated zircon grains from the Mount Elizabeth Granite, picked for clarity and absence of micro-fractures, define weighted average age of ca. 418.6 ± 2.6 Ma in the polished run.

Due to the overlap between the 2σ error envelopes for the results of in situ monazite and separated monazite and zircon studies, an average age of 417.30 ± 0.96 Ma (95% confidence) is assigned as the best crystallization age of the Mount Elizabeth Granite.

ACKNOWLEDGMENTS

This research represents part of a Ph.D. project completed at the University of New Brunswick. This project was financed in part by the Geological Survey of Canada as a part of the Targeted Geoscience Initiative (TGI4) program, and by a grant from Natural Resources Canada, and a Natural Sciences and Engineering Research Council (NSERC) discovery grant to D.R. Lentz, and Christopher McFarlane. The authors thank the many people and organizations who support this Ph.D. research. In particular, we thank Dr. Neil Rogers of the Geological Survey of Canada and the staff of the New Brunswick Department of Energy and Mines. We thank Jim Walker, Reginald Wilson, an anonymous reviewer, and journal editor Sandra Barr for their constructive reviews that led to improvement of this manuscript.

REFERENCES

Aleinikoff, J. N., Schenck, W.S., Plank, M.O., Srogi, L., Fanning, C.M., Kamo, S.L., and Bosbyshell, H. 2006. Deciphering igneous and metamorphic evens in high-grade rocks of the Wilmington Complex, Delaware: Morphology, cathodoluminescence and backscattered electron zoning, and SHRIMP U-Pb geochronology of zircon and monazite. Geological Society of America Bulletin, 118, pp. 39–64. http://dx.doi.org/10.1130/B25659.1

Anderson, T. 2002.Correction of common lead in U–Pb analyses that do not report ^{204}Pb. Chemical Geology, 192, pp. 59–79. http://dx.doi.org/10.1016/S0009-2541(02)00195-X

Azadbakht, Z, Lentz, D.R, and McFarlane, C. 2015. Using biotite composition of the Devonian Mount Elizabeth Intrusive Complex, New Brunswick, as a proxy for magma fertility and differentiation in W-Mo-Au-Sb mineralized magmatic hydrothermal systems. Atlantic Geology, 51, p. 106–107. http://dx.doi.org/10.4138/atlgeol.2015.005

Bevier, M.L. and Whalen, J.B. 1990. U-Pb geochronology of Silurian granites, Miramichi terrane, New Brunswick. *In* Radiogenic age and isotopic studies, Report 3. Geological Survey of Canada, Paper 89-2, pp. 93–100.

Chappell, B. W., Bryant, C. J., Wyborn, D., White, A. J. R., and Williams, I.S. 1998. Hot and low temperature I-type granites. Resource Geology, 48, pp. 225–235. http://dx.doi.org/10.1111/j.1751-3928.1998.tb00020.x

Chowdhury, S. and Lentz, D.R. 2011. Mineralogical and geochemical characteristics of scheelite-bearing skarns, and genetic relations between skarn mineralization and petrogenesis of the associated granitoid pluton at Sargipali, Sundergarh District, Eastern India. Journal of Geochemical Exploration, 108, pp. 39–61. http://dx.doi.org/10.1016/j.gexplo.2010.07.005

Christiansen, E.H. and Keith, J.D. 1996. Trace-element systematics in silicic magmas: a metallogenic perspective. *In* Trace Element Geochemistry of Volcanic Rocks: Applications for Massive Sulfide Exploration. *Edited by* D.A. Wyman. Geological Association of Canada, Short Course Notes 12, pp. 115–15.

de Roo, J. A. and van Staal, C.R. 1994. Transpression and extensional collapse: Steep belts and flat belts in the Appalachian Central Mobile Belt, northern New Brunswick, Canada. Geological Society of America Bulletin, 106, pp. 541–552. http://dx.doi.org/10.1130/0016-7606(1994)106<0541:TAECSB>2.3.CO;2

Fyffe, L.R. 1971. Geology of Forks of Nepisiguit and South Branch, New Brunswick (map-area M-8), New Brunswick Department of Natural Resources, Map Plate 71-45, 1:50 000 scale.

Fyffe, L.R., Pajari, G.E., and Cherry, M.E. 1981. The Acadian plutonic rocks of New Brunswick. Maritime Sediments and Atlantic Geology, 17, pp. 23–36. http://dx.doi.org/10.4138/1373

Fyffe, L.R., Johnson, S.C, and van Staal, C.R. 2011. A review of Proterozoic to Early Paleozoic lithotectonic terranes in the northeastern Appalachian orogen of New Brunswick, Canada, and their tectonic evolution during Penobscot, Taconic, Salinic, and Acadian orogenesis. Atlantic Geology, 47, pp. 211–248. http://dx.doi.org/10.4138/atlgeol.2011.010

Harrison, N. B., Pearce, J. A., and Tindle, A. G. 1986. Geochemical characteristics of collision-zone magmatism. *In* Collision Tectonics. *Edited by* M.P. Coward and A.C. Ries. Geological Society, London, Special Publications, 19, pp. 67–81.

Harrison, T.M., Aleinikoff, J.N., and Compston, W. 1987. Observations and controls on the occurrence of inherited zircon in Concord-type granitoids, New Hampshire. Geochimica et Cosmochimica Acta, 51, pp. 2549–2558. http://dx.doi.org/10.1016/0016-7037(87)90305-X

Klotzli, U.S., Koller, F., Scharbert, S., and Hock, V. 2001. Cadomian lower-crustal contributions to Variscon granite petrogenesis (south Bohemian pluton, Austria): constrains from zircon typology and geochronology, whole rock, and feldspar Pb-Sr isotope systematics. Journal of Petrology, 42, pp. 1621–1642. http://dx.doi.org/10.1093/petrology/42.9.1621

Ludwig, K. 2009. SQUID 2: A User's Manual. Berkeley Geochronology Center Special Publication 5, 110 p. URL <http://www.bgc.org/isoplot_etc/squid/SQUID2_5Manual.pdf> January, 2016.

McFarlane, C.R.M. 2015. A geochronological framework for sedimentation and Mesoproterozoic tectono-magmatic activity in lower Belt-Purcell rocks exposed west of Kimberley, BC. Canadian Journal of Earth Sciences, 52, pp. 444–465. http://dx.doi.org/10.1139/cjes-2014-0215

McFarlane, C.R.M. and Luo, Y. 2012. U-Pb geochronology using 193 nm Excimer LA-ICP-MS optimized for in situ accessory mineral dating in thin sections. Geoscience Canada, 39, pp. 158–172.

New Brunswick Department of Energy and Resource Development. 2016. New Brunswick Bedrock Lexicon. URL <http://dnr-mrn.gnb.ca/Lexicon/Lexicon/Lexicon_Search.aspx?lang=e> May, 2016.

Paces, J.B. and Miller, J.D. 1993. Precise U-Pb Ages of Duluth Complex and related mafic intrusions, northeastern Minnesota - geochronological insights to physical, petrogenetic, paleomagnetic, and tectonomagmatic processes associated with the 1.1 Ga Midcontinent Rift System. Journal of Geophysical Research-Solid Earth, 98, pp. 13997–14013. http://dx.doi.org/10.1029/93JB01159

Paton, C., Hellstrom, J.C., Paul, B., Woodhead, J.D., and Hergt, J.M. 2011. Iolite: Freeware for the visualisation and processing of mass spectrometric data. Journal of Analytical Atomic Spectrometry, 26, pp. 2508–2518. http://dx.doi.org/10.1039/c1ja10172b

Pearce, J. 1996. Sources and settings of granitic rocks. Episodes, 19, pp. 120–125.

Pearce, J. A., Harris, N. B., and Tindle, A. G. 1984. Trace element discrimination diagrams for the tectonic interpretation of granitic rocks. Journal of petrology, 25, pp. 956–983. http://dx.doi.org/10.1093/petrology/25.4.956

Petrus, J.A. and Kamber, B.S. 2012. VizualAge: A novel approach to laser ablation ICP-MS U-Pb geochronology data reduction. Geostandards and Geoanalytical Research, 36, pp. 247–270. http://dx.doi.org/10.1111/j.1751-908X.2012.00158.x

Roddick, J.C. and Bevier, M.L. 1995. U-Pb dating of granites with inherited zircon: conventional ion microprobe results from two Paleozoic plutons, Canadian Appalachian. Chemical Geology (Isotope geoscience section), 119, pp. 307–329. http://dx.doi.org/10.1016/0009-2541(94)00107-j

Rollinson, H.R. 1993. Using geochemical data: evaluation, presentation, interpretation. Longman Scientific and Technical, London, 352 p.

Schoene, B. 2014. U-Th-Pb Geochronology. *In* Treatise on Geochemistry, Second Edition, 4.10. *Edited by* H. Holland and K. Turekian, Elsevier, p. 341–378.

Shand, S.J. 1943. Eruptive rocks: their genesis, composition, classification, and their relation to ore deposits (Second Edition). John Wiley and Sons, New York, 444 p.

Sláma, J., Košler, J., Condon, D. J., Crowley, J. L., Gerdes, A., Hanchar, J. M., Horstwood, M.S.A., Morris, G.A., Nasdala, L., Norberg, N., Schaltegger, U., Schoene, B., Tubrett, M.N., and Whitehouse, M. J. 2008. Plešovice zircon—a new natural reference material for U–Pb and Hf isotopic microanalysis. Chemical Geology, 249, pp. 1–35. http://dx.doi.org/10.1016/j.chemgeo.2007.11.005

Sun, S. S. and McDonough, W. S. 1989. Chemical and isotopic systematics of oceanic basalts: implications for mantle composition and processes. Geological Society of London, Special Publications, 42, pp. 313–345. http://dx.doi.org/10.1144/GSL.SP.1989.042.01.19

van Staal, C.R., Whalen, J.B.,Valverde-Vaquero, P., Zagorevski, A., and Rogers, N. 2009. Pre Carboniferous, episodic accretion-related, orogenesis along the Laurentian margin of the northern Appalachians. Geological Society of London Special Publications 327, pp. 271–316. http://dx.doi.org/10.1144/SP327.13

Watson, E.B. and Harrison, T.M. 1983. Zircon saturation revisited: temperature and composition effects in a variety of crustal magma types. Earth and Planetary Science Letters, 64, pp. 295–304. http://dx.doi.org/10.1016/0012-821X(83)90211-X

Whalen, B.J. 1993. Geology, petrography, and geochemistry of Appalachian granites in New Brunswick and Gaspésie, Quebec. Geological Survey of Canada, Bulletin No. 436, 124 p. http://dx.doi.org/10.4095/183907

Whalen, J.B., Jenner, G.A., Longstaffe, F.J., and Hegner, E. 1996. Nature and evolution of the eastern margin of Iapetus: geochemical and isotopic constraints from Siluro-Devonian granitoid plutons in the New Brunswick Appalachians. Canadian Journal of Earth Sciences, 33, pp. 140–155. http://dx.doi.org/10.1139/e96-014

Whalen, J. B., McNicoll, V. J., van Staal, C. R., Lissenberg, C. J., Longstaffe, F. J., Jenner, G.A. and van Breemen, O. 2006. Spatial, temporal and geochemical characteristics of Silurian collision-zone magmatism: An example of a rapidly evolving magmatic system related to slab break-off. Lithos, 89, pp. 377–404. http://dx.doi.org/10.1016/j.lithos.2005.12.011

Wilson, R.A. (Compiler) 2013a. Geology of the Nepisiguit Lakes area (NTS 21 O/07), Northumberland and Restigouche counties. New Brunswick Department of Energy and Mines, Geological Surveys Branch, Map Plate 2013-11, 1:50 000 scale.

Wilson, R.A. (Compiler) 2013b. Geology of the California Lake area (NTS 21 O/08), Northumberland and Gloucester counties, New Brunswick. New Brunswick Department of Energy and Mines, Geological Surveys Branch. Map Plate 2013-12, 1:50 000 scale.

Wilson, R. A. and Kamo, S., 2008, New U-Pb ages from the Chaleurs and Dalhousie groups: implications for regional correlations and tectonic evolution of northern New Brunswick. *In* Geological Investigations in New Brunswick for 2007. Edited by G.L. Martin. New Brunswick Department of Natural Resources; Minerals, Policy and Planning Division Mineral Resource Report 2008-1, pp. 55–77.

Wilson, R. A. and Kamo, S. L. 2016, Geochronology and lithogeochemistry of granitoid rocks from the central part of the Central plutonic belt, New Brunswick: implications for Sn-W-Mo exploration. Atlantic Geology, 52, pp. 125–167. http://dx.doi.org/10.4138/atlgeol.2016.007

Yang, X.M. 2005. Petrogenesis of gold-related granitoid intrusions in southwestern New Brunswick, Canada. Unpublished Ph.D. thesis, University of New Brunswick, Fredericton, New Brunswick, 428 p.

Yang, X. M., Lentz, D.R., Chi, G., and Thorne, K.G. 2008. Geochemical characteristics of gold-related granitoids in southwestern New Brunswick, Canada. Lithos, 104, pp. 355–377. http://dx.doi.org/10.1016/j.lithos.2008.01.002

Editorial responsibility: Sandra M. Barr

APPENDIX A

Table A1. Mineralogical composition of analyzed samples from the SNRPS taken from Whalen (1993).

Unit	Sample number	Quartz	Plagioclase	K-feldspar	Olivine	Pyroxene	Amphibole	Biotite	Muscovite	Opaque minerals	Titanite	Allanite	Apatite	Zircon
Mount Elizabeth Granite	WX85NB-74	32.8	41.7	17.8				7.2	0.5					
	WX85NB-80	32.3	29.2	34.3				4						0.2
	WX85NB-81	30.4	43.8	21.9				3.8	0.1					
	WX85NB-95	25.7	36.3	31				6.8					0.2	
	WX86NB-240	31.6	25.1	40.7				2.3	0.1	0.3				
	WX86NB-250	32.7	32	30.5				4.7				0.1		
	WX87NB-325	28	33	29.2				9.4	0	0.1				0.2
Mount LaTour Granite	WX86NB-254	29.5	27.1	34.3				8.4		0.6		0.1		0.1
	WX86NB-262	39	4.1	53			0.5	2.3		0.6	0.2	0.1		0.2

APPENDIX B

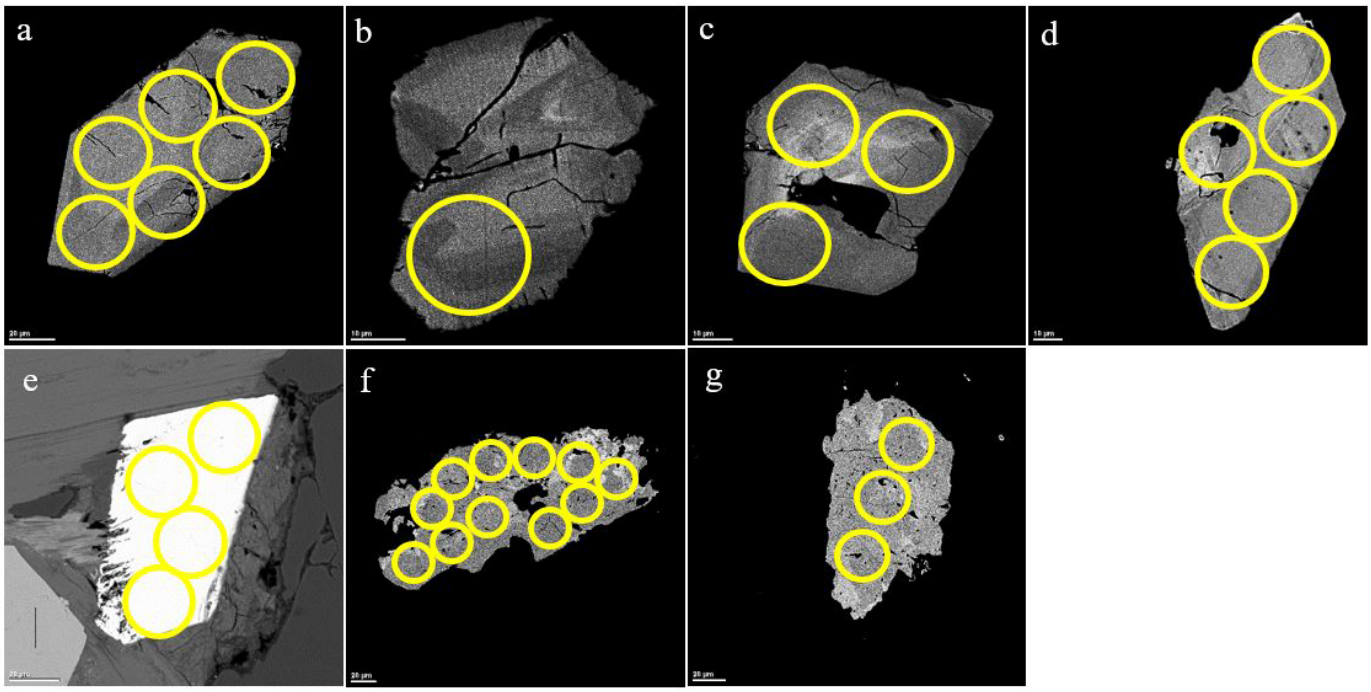

Figure B1. Enhanced-contrast BSE-SEM images showing compositional zoning and laser beam spots in monazite grains from two of the studied samples from the South Nepisiguit River Plutonic Suite. (a to f) grains from WX86NB-240 (Mount Elizabeth Granite) and (g, h) grains from WX86NB-254 (Mount LaTour Granite).

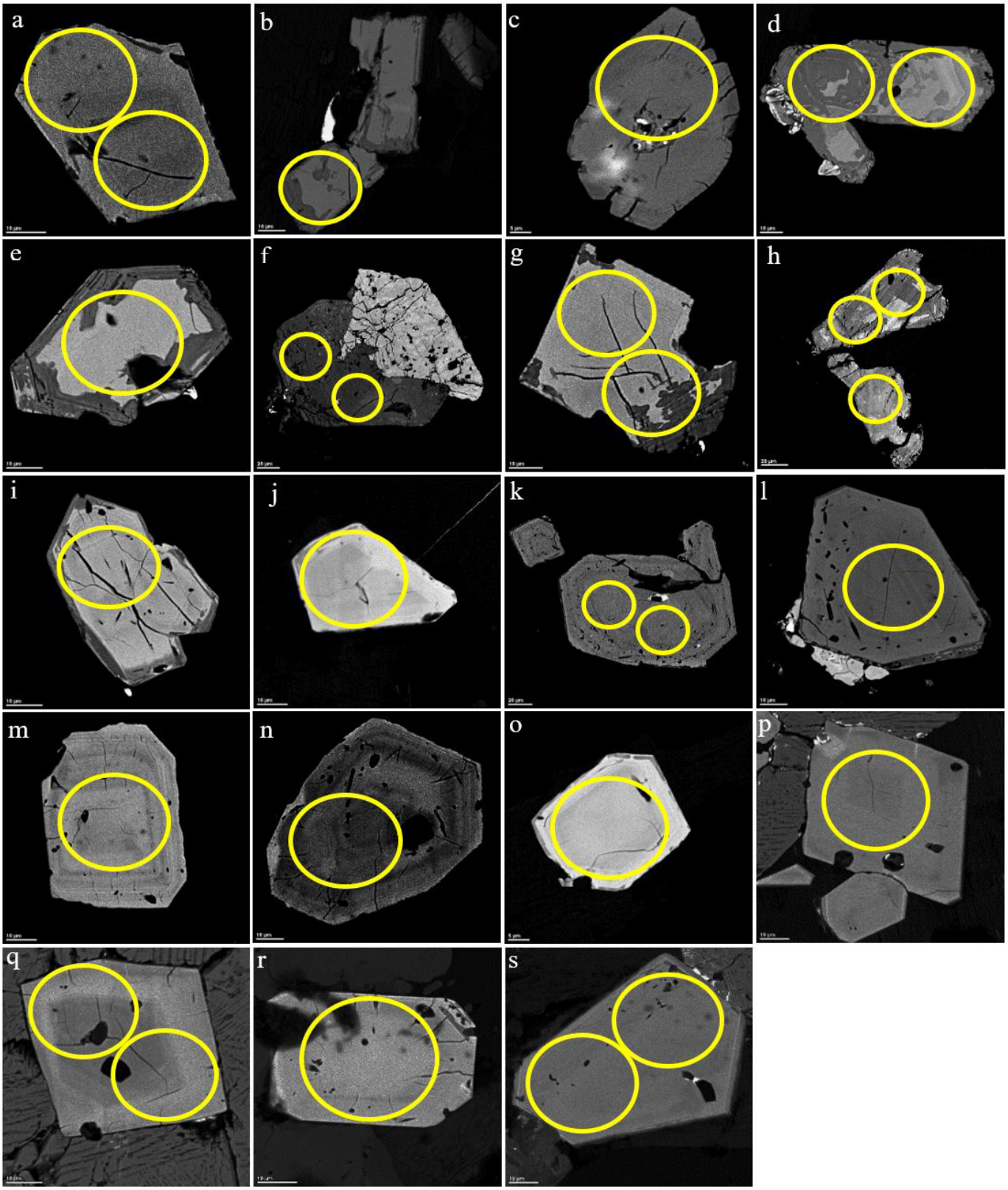

Figure B2. Enhanced-contrast BSE-SEM images showing compositional zoning and laser beam spots in zircon grains from three of the studied samples from the South Nepisiguit River Plutonic Suite. (a to h) grains from WX86NB-240, (i to o) grains from WX86NB-254, and (p to s) from WX86NB-262.

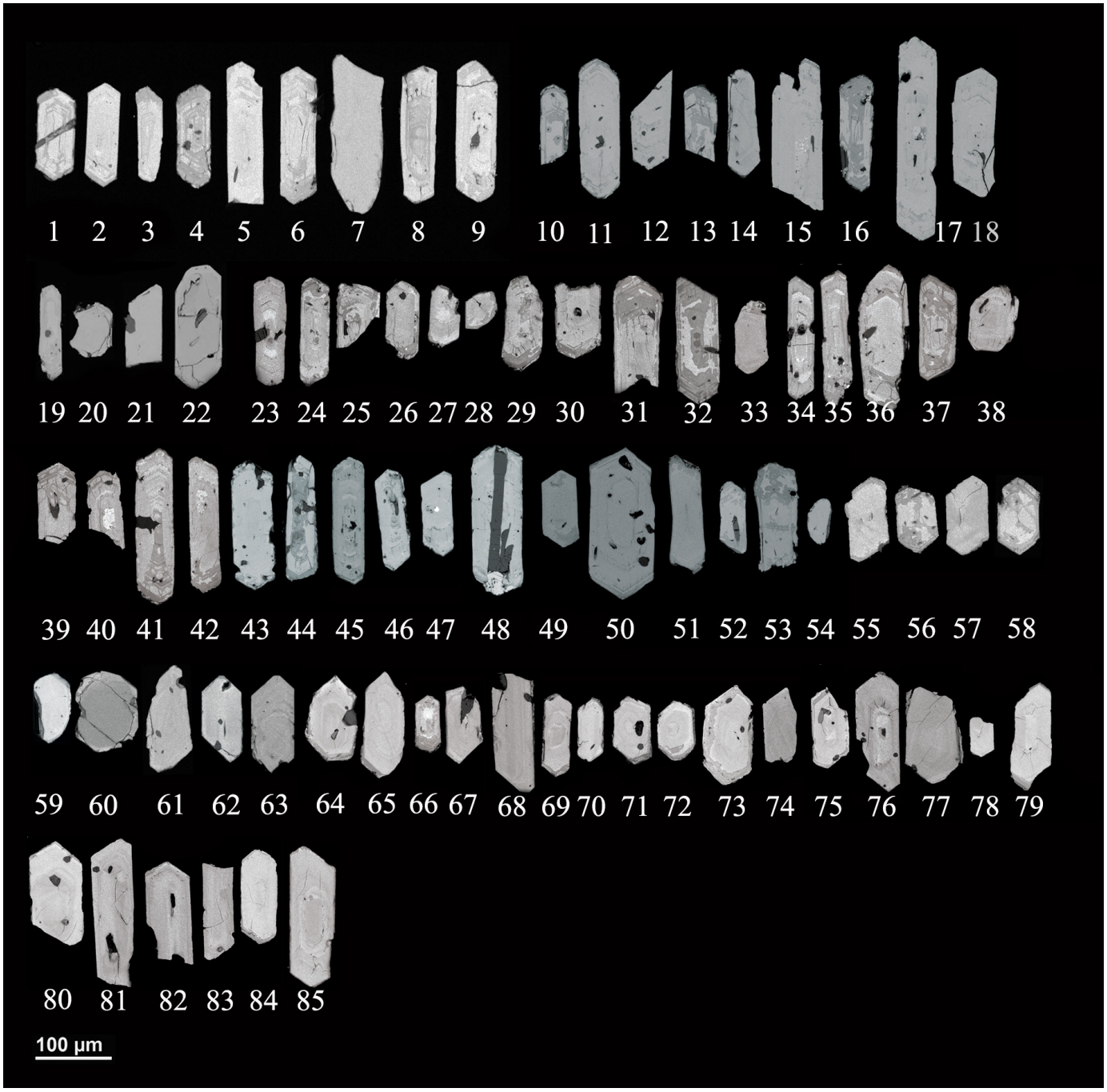

Figure B3. Enhanced-contrast BSE-SEM images showing compositional zoning in separated zircon grains from seven samples of the Mount Elizabeth Granite. (1 to 9) from WX85NB-74, (10 to 18) from WX85NB-80, (19 to 22) from WX85NB-81, (23 to 48) from WX85NB-95, (49 to 54) from WX86NB-240, (55 to 62) from WX86NB-250, and (63 to 85) from WX87NB-325.